

***A STUDY OF THE CURRENTS OF THE OUTER SHELF AND UPPER
SLOPE FROM A DECADE OF SHIPBOARD ADCP OBSERVATIONS IN
THE MIDDLE ATLANTIC BIGHT***

C. N. Flagg¹, M. Dunn^{1†}, D.-P. Wang¹, H. T. Rossby², and R. L. Benway³

Published in
J. Geophys. Res.
[vol. 111, C06003, doi:10.1029/2005JC003116]

June 2006

[†] Atmospheric Sciences Division, Brookhaven National Laboratory, Upton, NY 11973-5000.

¹ Marine Science Research Center, Stony Brook University, Stony Brook, NY 11794-5000.

² Graduate School of Oceanography, University of Rhode Island, Kingston, RI 02881.

³ Northeast Fisheries Science Center Narragansett Laboratory, Narragansett, RI 02882.

**Environmental Sciences Department
Atmospheric Sciences Division**

Brookhaven National Laboratory

P.O. Box 5000
Upton, NY 11973-5000
www.bnl.gov

Abstract

Since 1992 upper ocean ADCP current data between New York and Bermuda have been gathered from the container ship *Oleander* to identify long-term changes in the shelf, slope, Gulf Stream and Sargasso Sea. Temperature and surface salinity data have been collected along this route since 1978 by NOAA/NMFR. The first ten years of the ADCP data from which the effects of warm ring have been removed are used to describe processes within the shelfbreak frontal sub-region. The Eulerian mean velocity structure shows an along-isobath shelfbreak jet with maximum speeds of $O(0.15 \text{ m s}^{-1})$ offshore of which is a $\sim 30\text{km}$ wide relatively quiescent region. There is also an offshore slope current 40 to 50 km wide extending vertically to 300 m, with similar velocities as those found in the shelfbreak jet. The mean shelfbreak jet transport is 0.4 Sv while the slope current adds another 2.5 Sv. Maximum shelfbreak transport occurs in the fall and winter while the slope current reaches its maximum during the spring. In stream coordinates, the shelfbreak jet has maximum speeds of 0.35 m s^{-1} , a width of $\sim 30\text{km}$ and a vertical decay scale of $\sim 50\text{m}$. The maximum Rossby number within the jet, defined by $|dU/dy|_{\text{max}}/f$, is about 0.2. Significant interannual fluctuations occur in upper ocean temperature, salinity and currents some of which appear related to changes in the NAO index. Seasonal changes in the slope current appear to be related to annual changes in the wind stress curl over the slope sea.

Introduction

The shelfbreak frontal system is an area subject to a long litany of processes, for many of which we have but rather incomplete ideas about their origin, energetics and consequences for the region despite several decades of effort. And yet the shelfbreak front is known, if only from large scale balances, to play a critical role as the gate keeper for the transfer of mass and dissolved or suspended material on and off the shelf. It is thus largely responsible for the enormous productivity of some 2000km of coast between Cape Hatteras and the Grand Banks. In this regard, the long period of shelfbreak observation afforded by the *Oleander* Project has provided an invaluable as well as an unprecedented view of the flow field in and around the shelfbreak front that can be used to further our understanding of this critical component of the coastal ocean. A dramatic illustration of the importance of the shelf water/slope water, or shelfbreak front to the coastal ecosystem was a figure (E. Horne personal communication) in about 1976 that showed where the Canadian Coast Guard had plotted the positions of foreign fishing vessels on the Scotian shelf. Except for a few stragglers making their way to and from port, all the vessels were located in the frontal zone. A scan of the distribution of many of the fish and squid species from the National Marine Fisheries trawl surveys (eg. Azarovitz and Grosslein, 1987) also emphasizes the high productivity of the area. This has been explained as a combination of a near continuous supply of new nutrients from below and offshore which together with the basic stratification of the shelfbreak front minimizing the effects of light limitation, promote high primary (Ryther and Yentsch, 1958; Marra et al., 1990; Ryan et al., 1999). In the Mid-Atlantic Bight the shelfbreak frontal average primary production is roughly 50% higher than that of either the mid-shelf or upper slope waters (O'Reilly et al., 1987).

The shelfbreak front itself is a relatively narrow region along the edge of the broad continental shelf where the fresher and lower density shelf waters are juxtaposed against the more saline and denser waters of the slope sea. The area has been studied for a long time (eg

Bigelow, 1993 and Bigelow and Sears, 1935), both because of its enhanced productivity and because of its critical role in the shelf eco-system. While the contrast between the adjacent waters masses on either side of the shelfbreak front over hundreds of kilometers attests to the strength of the dynamics responsible for its formation, large scale property balances indicate that there is considerable transfer of material through the front (Biscaye et al, 1994). Thus, a mass and salinity balance in the Middle Atlantic Bight indicates that approximately three quarters of the water that passes south of Nantucket leaves the shelf by the time it reaches Delaware and a third of the water that is lost is replaced by the more saline waters of the upper slope. Clearly this exchange involves a considerable amount of nutrients and suspended and dissolved organic material. Precisely how this is done and which processes are responsible for what portion of the exchange has not been satisfactorily documented as yet.

Intensive studies since the 1970's, all with the goal of understanding the dynamics of the front and the critical shelf and slope exchange processes, have been carried out using moorings and hydrographic surveys at various locations and for varying durations (NESDE, Beardsley and Flagg, 1976; NSF, Beardsley et al, 1985; SEEP-I, Walsh et al., 1988; SEEP-II, Biscaye et al. 1994; OMP, Verity et al., 2002; CMO/PRIMER, Dickey and Williams, 2001). In addition, there have been several smaller programs aimed at studying frontal meanders and eddies (Ramp et al., 1983; Garvine et al., 1988, 1989). The hydrography of the shelfbreak region has been described in a number of syntheses, the latest of which is that by Linder and Gawarkiewicz (1998) based upon the Hydrobase system (Curry, 1996) for portions of the Middle Atlantic Bight. A difficulty common to almost all these efforts is that the on and offshore motion of the front has made interpreting the moored Eulerian data difficult while the episodic nature of shipborne observations leads to problems forming statistically significant description of the frontal structure.

Current theory suggests that the formation of the front is a result of a complex interplay between upstream (Chapman et al, 1986; Loder et al., 1998) and nearshore (see Beardsley and Boicourt, 1981) sources of relatively buoyant equatorward flowing waters that form a bottom boundary layer with an offshore transport. This offshore, near-bottom transport ultimately breaks away from the bottom and upwells into the interior at an isobath that depends upon the total alongshore transport (Chapman, 1986, 2002; Chapman and Lentz, 1994, 1997; Gawarkiewicz and Chapman, 1991, 1992; Yankovsky and Chapman, 1997). The role of convergence in the front clearly plays a major role in the cross-frontal density contrast and the convergence within the bottom boundary layers from either side of the foot of the front has been well demonstrated by the dye release studies of Houghton (1995, 1997), Houghton and Visbeck (1998) and the turbidity plume clearly visible in the SEASOAR sections of Barth et al (1998, 2004). What has not been well documented to date is whether there is convergence in the upper part of the frontal zone although Frantantoni et al (2001) did observed an upper layer convergence they ascribed it to the downstream convergence of the isobaths. In the present study this upper jet convergence is convincingly documented and does not appear related to isobath convergence.

Since geostrophic calculations as well as moored current measurements show that the shelfbreak front forms a surface intensified jet it has long been a question as to what degree this jet is barotropically or baroclinically stable. Implicit is the idea that if it is unstable, how is the jet maintained in the face of the instability. Flagg and Beardsley (1978) took an early look at this problem with a channel model that suggested that while the shelfbreak appeared to be unstable, the growth rates were much too slow to be significant. Gawarkiewicz (1991) attacked the problem with an improved model that suggested seasonal (stratification) dependent growth rates

but still with e-folding times that were only marginally of significance to the shelf. The latest attempt to address this issue is that of Lozier et al., (2002) in which perturbations of a continuously stratified front are investigated. This time, the instability e-folding times for fronts that resemble those in the Middle Atlantic Bight have decreased to as little as a day depending upon the vertical and horizontal shears, and the scale of the jet. However, there are no particularly unstable wavelengths, simply shorter waves are more unstable than longer waves. This, plus the fact that the theory is for infinitesimal disturbances, makes it difficult to use the results to either identify or predict the existence of a frontal meander that results from an instability. Nevertheless, it is important to bear these results in mind when examining the structure of the front to see whether new information alters the potential that frontal instabilities could play a major role in the behavior of the front and the exchange of mass and material between shelf and slope.

One of the purposes of the *Oleander* project has been to provide enough observations of the shelfbreak frontal structure and its surroundings, over a long enough period of time, that it would be possible to form statistically meaningful descriptions of the front at seasonal and longer time scales. As many observations have shown, the shelfbreak front is an extremely dynamic feature which makes long-term observations such those made possible by the use of VOS vessels like the *Oleander* particularly valuable if we are to make progress in these critical regions.

The organization of the paper is as follows. The acquisition of the ADCP data and the issues associated with qualifying and selecting that portion of the data best suited to an analysis of shelfbreak front and upper slope currents are discussed first. We then discuss some of the salient features of the currents from this area with emphasis on the enormous variability that appears to be characteristic of the area. The mean structure of the shelfbreak jet is then developed using both a fixed Eulerian frame of reference and also in terms of a stream following coordinate system. The annual signal in the shelfbreak front and upper slope is then illustrated followed by a description of the interannual current variability and its relation to the long-term upper ocean temperature and salinity fluctuations. A summary and discussion follows in which is discussed some of the dynamical issues associated with the interaction of the shelfbreak jet and waters of the slope sea gyre.

The Data Set

The data for this study comes from a long-term velocity measurement project utilizing the container ship, the CMV *Oleander* operated by Bermuda Container Lines servicing Bermuda from Port Elisabeth, New Jersey. The ship is 118m long with a beam of 20m and a draft at the stern when loaded of 5.2m, 0.6m less at the bow. The *Oleander* makes weekly round trips between Elizabeth, NJ and Bermuda. The NOAA/NMFSC VOS program has been utilizing this vessel and its predecessor since 1978 to obtain monthly XBT, surface salinity and CPR samples across the shelf slope front. Under the auspices of the ADCP velocity measurement program, the XBT data collection effort has been extended southward across the Gulf Stream. The velocity data collection program was initiated in 1992. The issues associated with actually collecting data on a commercial ship are myriad and discussed in Flagg et al. (1997). A 150kHz RD Instruments narrow-band acoustic Doppler current profiler was installed in the ship near the centerline approximately 45m aft of the bow. Unlike most research vessels, the *Oleander* has no external keel and the bottom is flat which at times, leads to bubble sweep-down problems.

The temporal/spatial resolution of the velocity data is based upon the sampling interval and the ship's speed. Once the ship has left port its normal cruise speed is about 16kts (8 m s^{-1}) while the ADCP sampling interval is five minutes, typical for narrow-band 150kHz ADCPs. This leads to a horizontal resolution of approximately 2.4km. Vertical resolution varies depending upon the water depth. Over the shelf in waters less than about 100m, 4m vertical sample bins are used with 4 to 6m pulses while in deeper waters 8m bins and 16m pulses are used. Data collection was controlled by the DAS 2.48 data acquisition system with a modification known as AutoADCP to allow autonomous data collection. The change between shallow and deep water configurations nominally occurs over the 100m isobath. The configuration change results in a small sampling gap on either side of the 100m isobath depending upon whether the ship is north or south bound. Another important aspect affecting the data collection is that the ship is typically more heavily laden on the south bound trip than when on the north bound return trip. This results in a draft change of approximately 1m which makes the north bound trips more susceptible to poor data return during periods of bad weather. The *Oleander* ADCP data have gone through an extensive quality assurance review. From the data that survived the screening, we extracted those profiles with percent goods greater than 80% that fell within the study area.

The focus of this study is on the area of the shelfbreak front so that the region of interest extends from the approximately the 70m isobath offshore along the *Oleander*'s route about a 160km to the southeast to nearly the 3000m isobath (Figure 1). As the figure shows, the ship tracks lie west of the Hudson Canyon along a western traffic lane on the southbound trip and along an eastern lane when north bound. The center of the eastern lane parallels Hudson Canyon about 9 km to the southwest of the deepest part of the Canyon while the western lane lies another 11km to the southwest. As the figure also shows, not all the tracks fit neatly in the traffic lanes. As a result we have also excluded those data that lay more than 15 km on either side of a line extending from Ambrose Light along the mean *Oleander* track. The net result of the data sorting is that for the period from 1992 through 2001, velocity data came from 545 transits of the frontal area, producing some 32,000 five minute averaged velocity profiles.

Over the shelf break and on the shelf the tidal currents have significant amplitudes (cf. Moody et al. 1984) which must be removed from the records if the focus of attention is on the similarly sized or smaller mean and low-frequency currents. With moored current data this is easily accomplished by low-pass filtering. For the space/time ADCP data a different approach is needed that can deal with the temporally and spatially scattered nature of the data collection. For significant amounts of data from repeated cruises Dunn (2002) developed a method that provides a set of observationally based barotropic tidal predictions by which the major surface tidal constituents can be removed from the observations. The scheme worked well on Georges Bank using data from some 80 cruises spread all over the Bank. This method was used to de-tide the *Oleander* ADCP data using the M_2 constituent which accounts for the majority of the tidal variance in the area (Moody, et al. 1984). The other tidal constituents are a fraction of the M_2 component, more difficult to estimate and have not been included when de-tiding the current data.

In addition to tides, meanders and warm rings from the Gulf Stream are highly energetic phenomena that can confound the details of the shelf/slope frontal region and need to be excluded from the analysis if and when the focus is on the structure of the front and slope sea as these areas are presumed to exist in the absence of external forcing. Even a cursory inspection of the velocity data from the *Oleander*'s ADCP shows numerous occasions when currents in excess

of 0.5 m s^{-1} , with usually large easterly components, occupy a substantial portion of the study area. To deal with this problem, we have made use of the U.S. Navy's historic Gulf Stream frontal analysis data, current versions of which are available on the web (www.nlmoc.navy.mil). Their tabulated data on location, size and orientation of warm rings based upon AVHRR photos extends back to 1991 although there was a large gap in the coverage in 1999. In the period from 1995 through 2001 approximately 2 rings passed through at least a portion of the study region each year, remaining in the area for about 20 days. Generally, rings are formed well to the east of the study area and propagate westward, Figure 2. There was considerable variability in the number of ring-affected days; as many as 87 in 2001 and none in 1996. There are also interannual changes in ring pathways such as a shift from relatively offshore tracks in 1996 and 1997 to a more onshore mean track in 1999 and 2000. This behavior is undoubtedly linked to the on-offshore movement of the Gulf Stream (see Rossby et al., 2005).

In an effort to minimize the effects of warm rings on the analysis, a ring filtering procedure was developed and applied to the ADCP data. U.S. Navy's NAVOCEANO NLANT observations consisted of three-day composite observations recorded daily. We examined a number of satellite photos to compare the Navy's ring position, size and orientation with what we would have estimated particularly in light of our need to eliminate, to the extent possible, all currents associated with the ring. In general, we agreed with the Navy's estimates but added an additional 25% to the size of the ring to account for ring edge effects. Since there were sometimes gaps because of clouds or some oceanographic event that obscured the temperature gradients associated with a ring, or in cases when the ring moved more than one diameter in a day, we interpolated the position of the ring center to fill in the gaps. Any ADCP data collected from a location within a ring region and less than 1.5 days from a ring observation date was flagged as likely to contain ring effects in the velocities and was removed. This filtering scheme removed 55% of the original ADCP data from the study area.

Even though the above procedure removed most of the effects of the warm rings, it did not remove all instances when the study area velocities were impacted by Gulf Stream effects. In 1999 there was 169 days when the Navy's frontal analysis was inactive. Also, even though we expanded the nominal ring sizes by 25%, that did not always cover some of the deformations of the rings nor some of the filaments associated with the ring. So a transect-by-transect examination was carried out, which by its nature was somewhat subjective, to remove observations with a clear warm-ring signature of high speed anti-cyclonic activity. In addition, some transects were removed because of relatively poor ADCP coverage. The total ring analysis and transect inspection process reduced the number of available transects from 1992 through 2001 from 545 to 282 and the number of profiles from about 32,000 to about 20,000. 170 transects were from south bound trips, 112 from north bound trips. The temporal/spatial data coverage was less complete during the early years of the program as difficulties with operating on a commercial ship were slowly overcome. In later years, the coverage was much better although there were times of greater ring/Gulf Stream impact as in 1999 and 2001 which caused substantial gaps in the frontal coverage.

To look at the vertical and horizontal data distribution, the data from the 282 culled sections were bin-averaged into $2 \text{ km} \times 8 \text{ m}$ bins and the number of transects that filled each bin counted. The results are shown in Figure 3 indicating both a downward and offshore decrease in available velocity data. The high returns in the shelf/slope frontal zone between about 150 and 190 km is primarily due to the high productivity of the area and the abundance of acoustic scatterers. Acoustic scatterers decrease with depth and also in the offshore direction in the less

productive region of the slope sea gyre. The two configuration change areas are also visible at 150 and 160 km.

It has been mentioned (eg. Gawarkiewicz, et al., 2004) that internal tides can have a significant effect on shipboard ADCP velocity data. To assess this issue we looked at the vertical shear variance based upon differences between adjacent 8m bins as indicators of internal wave activity. It is very difficult to identify internal waves in this way on individual sections but when the shear profiles from all the sections were averaged together a recognizable pattern did emerge. There was enhanced shear activity in the on-offshore velocity component near the bottom in the area where the bottom parallels possible ray-paths of M_2 internal tides. Similar but smaller shear activity was also visible where one might anticipate ray paths to intersect the surface and bottom as the internal tides propagated onshore. However, the largest shear variances, $O(2 \times 10^{-5} \text{ sec}^{-2})$, were around 140km from Ambrose Light and inshore of the mean position of the shelfbreak jet. This area of high shear variance probably reflects the presence of higher frequency internal waves as well as internal tides. The results suggest that while internal tides may indeed impact individual transects, they do not appear to have a significant impact on discussions below which combine the results from numerous sections.

Description of the ADCP sections

Before proceeding with a statistical analysis of the velocity sections it is useful to explore some of the features of the best quality de-ringed data from the shelf/slope frontal area. Perhaps the most important aspect of the velocity and surface temperature data to note is how variable the shelf/slope frontal jet appears to be, at least in terms of its velocity signature. The near surface thermal structure associated with the front as recorded by the ADCP, is almost always there although a simple monotonic offshore increase in temperature is rarely evident. More usually, there are one or more areas of lower temperatures and these are generally associated with westward along-shelf flow features. Out of the 282 culled sections, only 50 to 70 clearly show an alongshore flow to the southwest in the vicinity of the shelf break. Actually, finding a section that matches most of the features that we commonly think of as the front is rather difficult. One example that illustrates the shelfbreak jet is shown in Figure 4 from a south bound section occupied on July 12, 1997 at a time during which, according the composite AVHRR photos from JHU/APL, the slope sea gyre was relatively quiescent. Here we see a surface intensified alongshore jet located over approximately the 150m isobath with maximum velocities of $\sim 0.25 \text{ m s}^{-1}$ that are associated with an offshore temperature gradient. The vertical extent of the jet in this example is roughly 50 m while farther offshore the currents are weakly toward the northeast. The offshore component in this section indicates a less intense onshore flow a feature that is quite common and one that is reflected in the mean section shown discussed below. The alongshore orientation of the currents is taken to be 225°T but determining the proper alongshore or along-isobath direction is always difficult as it depends both upon time and spatial scale of the processes involved.

Figure 5 shows another example of the frontal current structure in which a single strong shelfbreak jet is evident. In this case the cross-front temperature gradient is very strong ($\sim 2.5^\circ\text{C}$ in 15 km) and localized over the region of highest velocities. Maximum observed detided alongshore currents in this section were 0.50 m s^{-1} . Although the location, speed and thermal structure of the frontal jet were much as anticipated, the slab-like extent of the highest currents suggests a more extensive density structure than that recorded by the surface temperatures. As

is often the case with shipboard ADCP data the deeper density structure is generally unavailable to provide a more complete picture of the dynamics behind the current observations.

In Figure 6 we show a sequential series of velocity sections that emphasizes another aspect of the shelf break jet, the enormous variability that seems to characterize the region. Even though the velocity structures vary, these sections represent an unusually coherent time series. The four sections are separated in time by 2, 5 and 9 days and while some jet characteristics remain, such as its location over the shelf break and the associated surface temperature minimum, there are large changes in maximum velocity, transport and vertical extent. Wind forcing during this period was minimal and contemporaneous AVHRR data are unavailable so ascribing a cause for the variability is difficult. The velocity structure for May 30, 1996 was quite remarkable with a surface intensified alongshore flow that had a maximum of 0.65 m s^{-1} and a transport between 140 and 200km and over a depth range between 14 and 206m of 1.16 Sv. Slightly less than two days later the maximum current had dropped to 0.39 m s^{-1} with a rather more expected transport of 0.42 Sv. As time progressed in the succeeding sections the maximum velocities dropped to 0.34 m s^{-1} and then 0.19 m s^{-1} while transports decreased to 0.24 Sv on June 6, 1996 and actually reversed to -0.26 Sv over the same cross-front area by the 15th of June. Note also that there was a very distinct surface temperature minimum associated with the shelf break jet during this period. This feature is not uncommon and perhaps owes its existence in this case to the very strong initial currents which advected colder surface waters from the east before they had a chance to warm.

Mean Velocity Structure

Mean along- and offshore velocity sections were generated using only those de-tided transects that were free, to the extent possible, of distortions due to warm rings. In order to combine the transects, the data along each were averaged into 2km x 8m bins with the amount of data available for each bin shown in Figure 3. The greatest data availability occurs over the edge of the shelf in the vicinity of the shelfbreak jet. The largest number of observations comes from the stretch between the 100 to 200m isobaths where the maximum number of observations in any bin was about 220 out of a possible 282 de-ringed transects. The number of available observations decreased from there in all directions and particularly with depth to less than 100 below 250m. The results of the averaging for the period between late 1992 through 2001 are shown in Figure 7a with the distribution of standard errors shown in Figure 7b. The mean alongshore velocities are all to the west ranging from zero to about 0.13 ms^{-1} in the center of the shelfbreak jet. The mean offshore velocity component ranged from near zero over the shelf to -0.06 to -0.08 ms^{-1} offshore and at depth. The standard errors for both components are less than 0.02 ms^{-1} everywhere above about 350m and more than $\sim 20\text{m}$ above the bottom, and less than 0.01 ms^{-1} in the core of the jet. As a result, the depiction of the mean velocities in Figure 7a appears to be a statistically valid description for this area.

The alongshore mean velocities show the shelfbreak jet in the anticipated location with a surface intensified velocity structure, spanning the 80 to 150m isobaths and centered over the $\sim 120\text{m}$ isobath with a vertical extent of some 60m and a mean width of about 30km. The maximum mean alongshore velocity was 0.13 ms^{-1} in the 8m bin centered at 26m. Presumably the alongshore velocity in the core of the jet would increase toward the surface. Both on and offshore of the jet, as well as along the bottom the mean velocities decrease to less than 0.05 ms^{-1} . The mean cross-isobath velocities in the vicinity of the shelfbreak jet are near zero indicating

the validity of the assumed along-isobath (225°T) orientation of the jet. Offshore of the jet for some 20 to 40km and extending downward to the maximum range of the ADCP there exists a wide area of reduced alongshore flow. This of course is anticipated from the canonical density structure of the shelfbreak region and the assumed thermal wind balance but it is not something that has been directly observed before. Perhaps the most intriguing aspect of the mean velocity section, because it was not something that was anticipated, is the broad area of southwestward flowing slope water extending down to roughly 300m located between 230 and 270 km from Ambrose Light. In terms of water depth, the core of this slope current lies roughly between the 2000 and 2500m isobaths. The maximum mean velocities here were just over 0.1 ms^{-1} and located subsurface at a depth of about 100m. This feature, as well as the area of low velocities between the shelfbreak jet and this slope current, is only visible because of the elimination of the warm rings from the data set. Prior to the removal of the rings the occasional presence of strong eastward currents from the northern portion of the rings resulted in mean velocities to the east and northeast over most of the area offshore of the shelfbreak front.

Another view of the mean velocities is afforded by looking down at the vertically averaged velocity vectors between 14 and 52m for each 2km bin, Figure 8. Also illustrated are the velocity ellipses which reflect all variability other than the tides. This view shows that the core of the shelf break jet lies just offshore of the 100m isobath, that there is a region of relatively lower currents just offshore of the shelfbreak jet and that farther offshore lies the slope current with velocities nearly equivalent to those in the shelfbreak jet. There is a rotation of the velocity vectors from nearly along isobath over the shelfbreak to rather more onshore in the slope current area. Thus, there is a region of convergence just offshore of the shelfbreak jet which, from the vertical sections of Figure 7a, appears to get closer to the shelfbreak with depth. The current ellipses indicate preferred axes of current variation and it would appear that significantly preferred orientations exist only for the areas on either side of the shelfbreak jet core where the ratios of major to minor ellipse axes are from 1.3 to 1.5. In both the core of the shelfbreak jet and well offshore the ratios of the ellipse axes are not much greater than 1. The amplitudes of the current ellipses reflect the current standard deviations and almost everywhere the standard deviations are larger than the means. Just offshore of the shelfbreak jet the ellipse amplitudes increase fairly abruptly although they indicate no preferred direction.

The vertically integrated alongshore transports and their cumulative integral proceeding offshore, Figure 9, give another aspect of the shelfbreak current structure. These transport estimates are based upon only that part of the water column sampled by the ADCP which means that neither near surface nor near bottom contributions to the transport are included. The vertically integrated transport is about $2 \text{ m}^2 \text{ s}^{-1}$ inshore of the shelfbreak jet but jumps up to 7 to $8 \text{ m}^2 \text{ s}^{-1}$ in the core of the jet and then climbs steadily to a maximum of $\sim 37 \text{ m}^2 \text{ s}^{-1}$ in the center of the slope current before tapering off somewhat farther offshore. Much of the cause for the increased transport offshore is of course due to the increased water depth. Although the mean current distribution indicates that the currents decrease in magnitude below about 350m, it is highly probable that the transport estimate would increase, perhaps substantially, if we could include waters deeper than 350 to 400m. Nevertheless, the structure of the transport is interesting in that it shows the tremendous impact that the upper slope waters have on the overall alongshore transport to the west and southwest. The cumulative alongshore transport emphasizes this point in that it shows that the shelfbreak jet is responsible for approximately 0.4 Sv while the slope current adds another 2.5 Sv for a total alongshore transport between 14 and 400m of nearly 3 Sv. If we estimate the added alongshore transport on the shelf, assuming a

mean current speed of $\sim 0.05 \text{ m}^2 \text{ s}^{-1}$ and a width of 100 km, the total shelf and shelfbreak transport is only $\sim 0.55 \text{ Sv}$, still considerably less than that of the upper slope.

Another way to look at the characteristics of the shelfbreak jet is to attempt to track the core of the jet as it oscillates across the isobaths and changes its orientation. This is the methodology used by Pickart (2000) for a single ADCP transect and Frantantoni et al. (2003) for eight cross-frontal ADCP surveys and it has the potential advantage of maintaining the spatial structure of the jet to some extent. We have applied this technique here by first, restricting the search area for the shelfbreak jet to the region between 130 and 200 km from Ambrose Light. As Figure 7a shows this region encompasses the mean location of the jet while excluding the usual location of the slope current. The velocity sections were then examined to identify those with more than 70% coverage in the upper 50m and more than 50% coverage in the upper 100m. Of the 282 warm-ring-free velocity sections, this left a total of 109 sections with sufficient coverage, 35 southbound sections and 74 northbound. This subset of available sections reflects the overall annual distribution with the fewest observations in winter and in September. We then defined the center of the shelfbreak jet as the location of the 2km x 8m bin on each section with the highest speed to the southwest. Despite the fact that the shelfbreak jet is usually assumed to be a surface intensified jet this is not always the case and plots of the on- offshore and vertical (above 200m) distributions of the center show considerable variation in the jet's location, Figure 10. That the location of the shelfbreak jet is not tightly constrained in either the horizontal or vertical dimension is a reflection of the great variability we see in the behavior of the jet. Figure 10 shows that the most likely cross-shelf location of the jet depends upon its vertical location in the water column with the deeper jet centers located preferentially farther offshore. 70% of the time the center of the jet was above 78m and 56% of the time the center was above 46m. If we look at the cross-shelf location of the jet found above progressively shallower depths (200, 100 and 50m), as in the left panel of Figure 10, the center of the distribution clusters more and more strongly about a single mode between 160 and 170 km from Ambrose Light. The water depths at this distance from Ambrose range between 120 and 140m.

If we use the selection criteria just described to determine which sections to include, the resulting mean shelfbreak jet structure in stream coordinates presents a rather different picture depending upon the allowed depth range for the jet center. If we use all the sections with sufficiently data coverage, including those with deep jet centers, the mean jet structure extends deep into the water column with essentially no offshore tilt of the center of the jet. While the evidence clearly suggests that the shelfbreak jet in all its manifestation does not always subscribe to our preconceived notions of the jet structure, it does not seem reasonable to include the less frequent instances of a deep jet in developing a mean description. It is quite possible that the conditions when a deep jet core exists may be the result of factors other than those responsible for the usual shelfbreak frontal structure. For this reason, only 70 sections where the high speed center of the jet was about 50m, out the 109 with sufficiently dense coverage, were used. The stream coordinate system was defined for each of these sections such that the downstream direction corresponded to the median direction of those velocities greater than 75% of the maximum velocity found in the southeast to northwest quadrant. Velocity data within 20 km on either side of the location of the maximum velocity were extracted from each section and averaged to show the mean down- and cross-stream structure of the shelfbreak jet. Cross-stream velocities are positive offshore. The results of this procedure are shown in Figure 11.

This view of the alongshelf current structure of the shelfbreak jet is remarkably similar to the Eulerian mean shown in Figure 7a except that the speeds are nearly three times as large. The

standard errors for the along-jet component are all an order of magnitude smaller than the mean velocity estimates except in the lower left corner where the presence of the bottom restricts the number of observations. In this view the maximum mean velocity of the jet is about 0.35 m s^{-1} in the 8m bin centered at a depth of 26m compared to the maximum Eulerian velocity of 0.13 m s^{-1} in Figure 7. The jet velocities taper symmetrically to each side with an e-folding distance of about 15 km yielding a width that is very similar to that shown in Figure 7. This e-folding width is 50% larger than that suggest by the mean hydrographic structure off New Jersey from the analysis of Linder and Gawarkiewicz (1998, Table 2) (hereafter referred to as L&G). By using only those sections in which the core of the jet was located above 50m the offshore tilt of the jet is preserved to some extent although it is poorly resolved by the 2km resolution of the data. The tilt of the core of the jet is 2 to 3 km over a vertical distance of about 40m for a slope of about 0.016, a value which is considerably steeper than that of the mean slope of the 34.5 isohaline off New Jersey, 0.003, as reported by L&G (their Figure 9). But this slope is about the same as the tilt of the jet in the upper 50m or so of the shelfbreak jet as determined from the eight ADCP sections analyzed by Frantantoni et al. (2001, their Figure 9). The vertical scale of the jet as represented by the depth over which the velocity decreases by $1/e$ is $\sim 50\text{m}$, or about the same as that reported by L&G. The along-jet transport for depths less than 100m and for velocities greater than 0.1 m s^{-1} was 0.27 Sv which increases to 0.43 Sv if one assumes that the shallowest observed velocities continue to the surface. This transport estimate is undoubtedly something of an under estimate of total shelf break transport as it assumes no farther velocity increase toward the surface. However it is similar to previous estimates of shelfbreak transports made using a combination of sporadic hydrographic sections and moored observations (Beardsley and Flagg, 1975; Beardsley et al., 1985; Frantantoni et al., 2001) but this estimate is significantly larger than that estimated from the mean shelfbreak hydrographic structure offshore New Jersey by L&G. The cross-jet velocity structure shows a coherent structure in the upper 40 to 50 m that reflects a strong convergence into the center of the jet. The cross-jet velocities in the upper portion of the jet are two to five times the standard errors and clearly significantly non-zero. The maximum offshore velocities in the 26m bins are about 0.04 m s^{-1} just inshore of the center of the jet and opposed by onshore velocities of about 0.01 m s^{-1} a few kilometers on the seaward side of the center of the jet. The divergence of the cross-jet component, dV/dy , is shown in the third panel of Figure 11 where the maximum convergence occurs just offshore of the center of the jet and is estimated to be about $-1 \times 10^{-6} \text{ s}^{-1}$. If the convergence in the center of the jet is integrated downward from 26 m, the center of the shallowest 8 m bin, the implied vertical velocity at 60 m is more than 50 m day^{-1} . Again, this is probably an underestimate of the integrated convergence and if one assumes that the same degree of convergence extends to the surface, the vertical velocity estimate at 60 m would be around 60 m day^{-1} , (0.07 cm s^{-1}).

The last panel of Figure 11 shows the relative vertical vorticity of the shelfbreak jet with strong negative vorticity along on the shoreward side with positive vorticity on the offshore side. The range of relative vorticities in the upper layers is from -0.23 to $0.22 \times 10^{-4} \text{ s}^{-1}$. Thus, at the latitude of the shelfbreak jet, the relative vorticities are about 0.23 times the planetary vorticity and the maximum Rossby number, as defined by Lozier et al. (2002) in their discussion of shelfbreak stability, $|dU/dy|_{\text{max}}/f$, is also about 0.23.

Seasonal Variability

The seasonal distribution of the available de-ringed ADCP data is not uniform. The best coverage is from March through August and then again from October until Christmas. The hiatus in September is partially due to bi-annual yard periods which have typically been scheduled then. There is also less coverage in the January and February period as sea conditions from winter storms cause bubble sweep-down under the ship effecting the ability of the ADCP to collect data.

In order to illustrate the seasonal dependence of the alongshore flow field in the shelfbreak region, Eulerian means were determined for four three-month intervals, December – February, March – May, June – August and September – November, Figure 12. Because there are fewer observations in each of the seasonal averages one expects that the uncertainty of the estimates to suffer to some extent. The standard errors for the alongshore component increase by about a factor of two to three over those shown in Figure 7b with the greatest uncertainty occurring in the winter means offshore of 230 km and below about 80 m. Elsewhere, the seasonal mean velocity estimates in the regions of the shelfbreak jet and slope current are all significantly larger than the associated standard errors.

Figure 12 shows that the shelfbreak jet accelerates in the fall and is strongest in the winter months with a maximum mean speed of over 0.2 m s^{-1} and a width of some 20 to 30 km. This is also a time when the shelfbreak jet's lateral and vertical extent also seems to be at a maximum. The intensity of the shelfbreak jet is a lot less in the spring and summer months with mean speeds barely more than 0.1 m s^{-1} . During the spring and summer the region of reduced southwestward flow just off the shelf in the overall mean as shown in Figure 7, expands enormously to a width of 50 to 60 km but is barely visible in the fall and winter. Offshore, the core of the slope current seems to increase from being barely resolved in the winter to its maximum in the spring with a width of $\sim 50 \text{ km}$, a vertical extent of at least 300 m and a maximum mean speed of $\sim 0.15 \text{ m s}^{-1}$. The slope current has minimum velocities during the summer and the increases in speed as a subsurface feature in the fall. The slope current's transition between fall and winter conditions is poorly resolved with the available data.

The seasonal signal of the upper layer currents (14 to 52 m) can also be decomposed into a mean plus a series of annual plus semi-annual sines for each 2 km distance bin. The results of this least-square analysis are shown in Figure 13 which shows that the seasonal alongshore signal accounts for approximately 10% of the total variance of the shelfbreak jet and for most of the area of the slope current. Inshore of the shelfbreak jet, that is for transect distances less than $\sim 150 \text{ km}$ from Ambrose Light, there is little seasonal variability. The shelfbreak jet itself is located between 150 and 190 km, see Figure 10, and this view shows that the maximum alongshore flow begins around yearday 320 and lasts through yearday 80, with a long hiatus during the spring and summer as Figure 15 suggested. Farther offshore there is a definite phase lag relative to the shelfbreak jet of the maximal southwestward alongshore flow of the slope current, centered about 250 km offshore. This view also suggests that the slope current begins to accelerate earlier inshore. For the offshore component, the seasonal variability explains substantially less of the current variance although it does exhibit a coherent structure. The on-offshore seasonal signal of the shelfbreak jet itself is rather small with slightly greater offshore components in the spring and fall. The slope current, however, shows a substantial on-offshore variability with a greater onshore flow during the winter through summer and a greater offshore bias during the early fall.

Interannual Variability

With the removal of the seasonal signal (see Figure 14 below), it is possible to estimate the correlation length scales in the cross-isobath direction for both the alongshore and offshore velocity components. For this purpose the mean upper layer (14 to 52 m) velocities with tides and seasonal dependences removed were computed for each de-ringed section. Correlations for lags between zero and 80 km were then computed for each section from which the mean lagged correlations and their standard errors were derived. The correlation standard errors were all about 0.02. The correlations for the two components are quite similar although the alongshore component has slightly higher correlations for lags less than ~15km and then more negative correlations for lags between roughly 30 and 60km. The cross-isobath correlation length scales, as indicated by the first zero crossings, are about 25 km for the alongshore component and 35km for the offshore component. The correlation length scale, as indicated by the e-folding distance ($\rho \equiv e^{-1}$), for both components was 15km.

Interest now turns to the interannual variability that occurs in the shelfbreak region. For this, low-frequency upper level (14 to 52 m) velocity anomalies were constructed by subtracting the upper level mean and seasonal signals, as illustrated in Figure 13, from each of the available de-tided and de-ringed velocity sections. Sixty-day averages were then formed for each 2 km distance interval which were then temporally smoothed further using a low-pass filter with a one year half-power point. The result of this process is shown in Figure 14 for both the along- and offshore components. The long-term variability in both components is substantial with standard deviations of about 0.05 m s^{-1} and ranges of roughly $\pm 0.2 \text{ m s}^{-1}$. At the same time, the plots appear both spatially and temporally coherent which lends credence to the general character of the long-term variability depicted. In the shelfbreak region, that is less than 200 km from Ambrose Light, there was an initial 3.5 year period of relatively little anomalous behavior. This changed markedly in the latter half of 1997, extending to the beginning of 1998, with an alongshore acceleration of the flow to the southwest accompanied by an increased offshore flow. There followed a period of reduced or eastward alongshore flow for about a year and then a second period of increased flow to the southwest in the first half of 2000. Except in the first couple of years of poorly resolved variability, there appears to be a difference of character and timing of events between the region of the shelfbreak jet, inshore of 180 to 200 km, and the area farther offshore. Thus, the two periods of accelerated southwestward flow in the shelfbreak region are not matched by similar events offshore. Rather, there is increased southwestward flow over the slope in late 1996 and the first half of 1997, again in the latter half of 1998 with a smaller slope event in the winter of 2000/2001.

These interannual variations in the shelfbreak region and over the slope do not appear to be caused by local atmospheric or buoyancy forcing but rather must be linked to processes on a much larger scale. A revealing view of the variability in the region is provided by the long-term hydrographic measurement program from the *Oleander* carried out by the NMFS/Northeast Fisheries Science Center. Since 1978 and continuing on to the present, volunteers have been riding the *Oleander* once a month dropping XBTs, collecting surface salinity samples and towing a continuous plankton recorder across the shelf and upper slope with a particular emphasis on the shelfbreak frontal region. Some of these data were first shown by Rossby and Benway (2000) where the focus was on the movement of the Gulf Stream. Here we focus instead on the long-term temperature and salinity variations over the shelf and slope looking for the distribution and

timing of anomalous water properties in the near surface. XBT temperatures at 10m and surface salinity data were binned into 10km intervals along the *Oleander* transect starting from about 15 km from Ambrose Light and extending some 470km offshore roughly to the mean position of the Gulf Stream. The interannual anomaly fields for temperature and salinity were formed by removing the mean and least square fitted annual plus semi-annual sines at each distance bin. The anomaly fields were then low-pass filtered with an 18-month half-power point to form the final smooth temperature and salinity anomalies shown in Figure 15.

The low-passed temperature and salinity anomalies over this 24 year period have ranges of $\pm 4^{\circ}\text{C}$ and ± 2 psu with standard deviations of 1.1°C and 0.5 psu, respectively. The correlation coefficient between the temperature and salinity anomalies is 0.57 so that warmer than usual temperatures are correlated with higher salinities. Although there is a tendency for density compensating variations in temperature and salinity, the temperature changes are not, on average, sufficient to neutralize the density changes due to the salinity variations. The mode II regression line between the anomalies has a slope of $1.73^{\circ}\text{C}/\text{psu}$ while the ratio of salinity contraction, β , to thermal expansion, α , for the mean temperature and salinities of region is $3.29^{\circ}\text{C}/\text{psu}$ so that there are substantial and large scale density changes over the shelf and slope on interannual time scales.

The most striking features of the temperature and salinity variations are that the anomalies appear, for the most part, coherent all the way across the shelf and slope in addition to the fact that temperature and salinity anomalies are highly correlated. There are several large anomalous events in which temperature and salinity increased or decreased across the entire region. Thus there was a cold period in 1982 followed by a warm and saline event in 1986. Then there was a period of five to six years with smaller scale variations followed by another warm saline period in 1994/1995 at the beginning of the *Oleander* ADCP observation period. This was followed by a cold/low salinity anomaly in late 1996 that spanned the area from the Gulf Stream's north wall all the way to New York. This cold event was also observed in Long Island Sound (R. Wilson, personal communication). In the shelf break and slope region a cold period was again present through 1998 while there was a farther lowering of salinity over the upper slope and shelf. This low salinity anomaly period in 1998 had salinities ~ 1.5 psu below normal and was the lowest relative salinity of the entire 24 year record. There was then a transition toward warmer temperatures and more moderate salinities on the shelf and upper slope in the latter part of 1999. The one time that there was a substantial difference between the shelf and slope was in 2000 when there was a significant warm and somewhat saline anomaly just north of the Gulf Stream with near normal temperatures and salinities over the shelf and shelfbreak. The situation reversed in 2002 with somewhat warmer temperatures on the shelf and upper slope with near normal temperatures offshore followed by another reversal in 2003.

In terms of the *Oleander* period, clearly the most significant set of events were the advent of the two cold/low salinity water pulses from mid-1996 through 1998. There is growing evidence that the Gulf Stream, the slope sea as well as the Gulf of Maine/Georges Bank system were all impacted by variations in the atmospheric circulation over the sub-polar regions. Smith et al. (2001), Drinkwater et al. (2005), Pershing et al. (2001) and Greene and Pershing (2003) have posited that the large drop in the winter NAO index in 1996 and the associated changes in atmospheric forcing over the Labrador Sea were responsible for the influx of cold/fresh Labrador Slope Water into the slope sea, up onto the Scotian Shelf and through the Northeast Channel into the Gulf of Maine in 1998. This event was first observed by the Canadians in the Cabot Strait, Banquereau Bank and Halifax sections (Drinkwater et al., 2005). An associated acceleration of

westward flow south of the Grand Banks was predicted for this period based upon TOPEX/POSEIDON measured sea level slopes (Hendry, 2001). Westward transports of ~ 15 Sv in that area were estimated for mid-1996 and early 1997. There was an even larger westward transport estimate for the winter of 1993/1994 of ~ 17 Sv. Rossby and Benway (2000) suggested that the behavior of the Gulf Stream south of New England was linked to the Labrador slope waters that flowed into the slope sea around the Tail of the Bank and this thermohaline thesis has been pursued by Rossby et al. (2005) in which is illustrated a ~ 100 km southward shift of the axis of the Gulf Stream beginning in mid-1995, peaking in 1998 before recovering to a more northerly position in 2000.

Prior to the appearance of cold water in the slope sea during 1997/1998 there was another event of a similar magnitude the year before, in late 1996, see Figure 15. In fact, the low temperature anomaly of 1998 was less evident on the shelf than that of 1996. In long-term salinity records from the Georges Bank region compiled from MARMAP, GLOBEC and other sundry cruises, (D. Mountain, personal communication) distinctly shows two separate low salinity (and presumably low temperature) events. Smith et al. (2001) showed the presence of low salinity water in the Northeast Channel during early 1996 that appeared to come primarily from the outer Scotian Shelf rather from the slope sea directly. The arrival of the cold, low salinity water in the Northeast Channel was preceded by increased freshwater transport into the Gulf of Maine south of Cape Sable. An interesting aspect of the 1996 event is that, if this was predominantly a shelf event, as compared to the NAO linked and slope dominated event of 1997/1998, there had to be an enormous amount of leakage of the cold, low salinity water through the shelfbreak front for it to appear essentially synchronously over both slope and shelf in the western slope sea some months later.

To what extent are the interannual temperature and salinity anomalies within the temporal and spatial coverage provided by the *Oleander* current observations related to variations in the alongshore flow? In this analysis, we make the reasonable presumption that colder, fresher and less dense waters originate in the eastern slope sea and that warmer, more saline and denser waters are either advected into the area from the west or generated locally through vertical and horizontal mixing processes with waters of Gulf Stream or sub-Gulf Stream origin. We also make the assumption that the shelfbreak jet and the slope current represent the primary pathways for the waters that alter the local hydrographic conditions. Based upon this hypothesis a plot of the near surface alongshore current, temperature and salinity anomalies from the core of the shelfbreak jet at 160 ± 10 km and the center of the slope current at 260 ± 10 km (see Figures 13 and 16) are plotted in Figure 16. The temperature and salinity anomalies axes have been inverted in the figure consistent with the premise that increased southwestward alongshore flow leads to lower temperatures and salinities.

As mentioned earlier, there are two low temperature, low salinity events that dominate the 1996 through 1999 time period. The first of these events peaked in the later part of 1996 with colder temperatures but somewhat higher salinity than the event in 1998 with marginally colder temperatures in the shelfbreak jet area than in the slope current. The 1998 event was the more saline of the two with relatively colder temperatures in the slope current. If it is assumed that these cold and fresh events are the result of horizontal advection then one would expect that the westward flow anomalies would lead the minimum temperatures and salinities and that minimum temperatures and salinities would occur approximately coincident with a halt to the anomalous southwestward flow. This indeed appears to be the case but it is not completely obvious how the interaction between the shelfbreak and slope happens. In 1996 the slope current

anomaly peaks at about 5 cm s^{-1} in April and subsides to normal in late fall while slope temperatures and salinities reach their minima in the fall suggesting that this was an advective event. However, the shelfbreak currents showed only a small increase in the alongshore currents at this time seemingly at odds with the strong temperature and salinity anomalies. This is also at odds with the conclusion of Smith et al. (2001) that the 1996 event in the Scotian Shelf and Georges Bank area was primarily a shelf and shelf edge event which they based upon the fact that there was scant evidence for cold low salinity water below the surface from a mooring in the Northeast Channel. The 1998 event exhibited colder temperatures over the slope than in the shelfbreak area although minimum salinities were about the same. Both temperature and salinity reached their minima in the slope before they do in the shelfbreak jet. The shelfbreak current anomaly leading up to this event was two to three times that found in the slope but in both places the current anomaly led the temperature and salinity anomalies by approximately ninety degrees.

There also were two warm saline events in the area in 1995 and 1999 with magnitudes that rivaled the cold-fresh influx during the intervening years. In the year leading up to the warm saline period of 1995 the current anomalies were negative, that is there was a decrease in the alongshore flow but it was not of large enough magnitude to reverse the mean flow. Rather there was simply a decrease in the alongshore flow of a few cm s^{-1} . The warm saline period of 1999 seems to have had a closer relationship with the current anomalies with an abrupt and substantial decrease in alongshore flow both in the shelfbreak jet and in the slope current. The reversal in the anomalous currents in the latter portion of 1999 coincided with the maximal temperatures and salinities both of which began to return to more normal values when the current anomalies increased toward the southwest again. Thus, it appears that to a large extent, the interannual and large scale water property fluctuations observed over the shelfbreak and inner slope are the result of variations in the alongshore flow and the advection into the area of waters from either the southwest or northeast.

Discussion

In this analysis we have taken the large *Oleander* data set and have focused on developing a primarily kinematic description of the shelfbreak front of the Middle Atlantic Bight over a wide range of time and cross-frontal space scales. Critical to the analysis has been the ability to eliminate more than half the transects due to contamination from Gulf Stream warm rings since the goal has been to describe to the extent possible, the characteristics of the shelfbreak front in the absence of external forcing.

Using the subset of ADCP data qualified in this manner we developed two descriptions of the mean shelfbreak jet. The Eulerian description showed a contained surface intensified mean jet with maximum speeds of $\sim 0.13 \text{ m s}^{-1}$ centered over the 120m isobath with a vertical extent of some 60m and a mean width of about 30km. The surprising thing that came out of the Eulerian description of the mean shelfbreak and upper slope currents was the appearance of an intense, spatially concentrated slope current that might qualify as a “slope jet”. The estimated along isobath transport of the shelfbreak jet, 0.4 to 0.5 Sv, generally agrees with the many past estimates but it was shown that these transports were dwarfed by the 2.5 Sv or greater transport of the upper slope current system. The description of the shelfbreak jet in terms of stream coordinates revealed other aspects of the frontal system. First, the maximum mean down-jet velocity in stream coordinates, 0.35 m s^{-1} was nearly three times larger than that indicated by the Eulerian mean. The horizontal and vertical e-folding scales of the jet in stream coordinates were

15 km and 50m, respectively. The estimated down-stream transport from this description, 0.3 to 0.4 Sv, was very similar to that of the Eulerian mean transport because while the maximum mean velocities were higher, the vertical extent was less. Particularly useful quantities from the stream coordinate description were estimates of a maximum upper layer convergence of $\sim 1 \times 10^{-6} \text{ s}^{-1}$ in the center of the jet and maximum relative vorticities of $\sim 0.2 \cdot f$ on either side of the jet core.

The seasonal variability of the shelfbreak jet is not an easy thing to define using conventional approaches because of the jets inherent synoptic scale variability. However, with ten years of ADCP data concentrated along a narrow track across the shelf we were able to derive statistically significant estimates of the seasonal flow field. The shelfbreak jet within the domain monitored by the ADCP appeared to accelerate in the fall with a clear annual maximum in winter and minimum velocities in the spring and summer. The seasonal cycle from the ADCP data agrees with estimates made by Linder and Gawarkiewicz (1998) for the waters off New Jersey based upon the seasonal mean hydrography but differs from their estimate for the front south of Nantucket in which the frontal jet appears to be stronger in the summer. The offshore slope current has its well defined maximum in the spring.

On interannual time scales the upper 50m currents and near surface temperature and salinities showed major fluctuations of order $\pm 0.2 \text{ m s}^{-1}$, $\pm 4^\circ\text{C}$ and $\pm 2 \text{ psu}$, respectively. The temperature and salinity variations were highly correlated and coherent all across the shelf and slope out to the Gulf Stream. The velocity variability across the frontal region was not as coherent as were the water properties and there were some differences between the response of the shelfbreak jet and the slope current. However, there was a clear relationship between the interannual current variations and the water properties indicating that the hydrographic variability was largely due to advective effects rather than in situ water mass formation processes. If the long-term variability is ultimately due to the thermohaline forcing at the slope sea boundaries (Rossby and Benway, 2000; Rossby et al., 2005) then there must have been some as yet unresolved precursor signal propagation that set up the internal density field to produce the currents leading to the water property changes. How this signal produced the coherent property changes in both the shelf and slope needs further study.

Despite the amount of details about the shelfbreak jet structure that has emerged from the ADCP and near-surface hydrographic data, we are still missing some important elements to form a more complete dynamical description. The two main difficulties are 1) the lack of data near the bottom where the dynamically important upwelling out of the bottom boundary layer occurs, and 2) the lack of contemporaneous frontal density information with which to examine the baroclinic balances. However, we have been able to document enough of the velocity structure to describe the cross-stream velocity structure. The mean jet in stream coordinates, Figure 11, shows a strong and coherent offshore flow on the inshore side of the jet in the upper 40 to 50m with a much smaller onshore flow on the offshore side. The convergence that results from the gradient in the cross-stream flow is on the order of $-1 \times 10^{-6} \text{ s}^{-1}$, resulting in a downwelling of about 50 m day^{-1} in the upper half of the water column. This presents an interesting counterpoint to the picture of upwelling out of the bottom boundary layer predicted by frontal models (Chapman, 2002) and observed in dye studies (Houghton and Visbeck, 1998) and turbidity plumes (Barth et al., 2004). Based upon observed dye movement along isopycnals of $2 \times 10^{-2} \text{ m s}^{-1}$ and a representative isopycnal slope of the front of 2×10^{-3} , the upwelling out of the bottom boundary layer occurs at a rate of roughly 3.5 m day^{-1} . So, if we have 50 m day^{-1} coming down from the upper part of the water column and 3.5 m day^{-1} rising out of the bottom boundary layer, what happens to the water that meets somewhere in the middle of the water column?

Presumably this convergence in the middle of the front results in flow either on or offshore. We do not know whether this converging water cycles back to the surface or bottom in a pair of line vortices, whether the accumulated waters deform the front and perhaps enhanced vertical mixing, or whether the water is expelled from the front either on or offshore. Is this a potential source of the expelled shelf water that passes through the front approximately along isopycnals in a process referred to as “calving” (Wright, 1976)?

Another area in which these result might be useful is assessing the potential for the development of frontal instabilities. The most current research on this issue is that of Lozier, Reed and Gawarkiewicz (2002) in which a linearized primitive equation description of insipient frontal meanders of a geostrophically balanced front jet was used to assess potential growth rates and propagation speeds. When applied to the Middle Atlantic bight and using shelfbreak jet parameters from previous studies the growth rates were fairly small, e-folding times of 2 to 4 days. If instead we assume characteristics similar to the mean in stream coordinates then, if we extrapolate to the surface, V_{\max} is $\sim 0.45 \text{ m s}^{-1}$, the maximum observed shear is $\sim 0.006 \text{ s}^{-1}$ and the Rossby number is ~ 0.23 . Assuming that the background stratification is as in their model runs, the shelfbreak jet parameters are very similar to their calculations.

One of the more intriguing results of this study is the seasonal presence of the concentrated slope current, or slope jet. This immediately begs the question of what is it? The quality of the data and error estimates clearly suggest that this is a real feature of the slope sea. If so it represents the first time that the slope sea has been characterized as anything other than a slow rather amorphous cyclonic by product of the Gulf Stream’s separation from the coast whose most dynamic elements were warm rings. This still leaves us with trying to explain the existence of this energetic and seasonally varying flow regime. Csanady and Hamilton (1988) presented a highly simplified theory of the slope sea gyre. Their model assumes a Sverdrup balance for most of the region in which the circulation is driven by a combination of wind stress curl and flow in and out of the boundaries. The flow into the slope sea represents the low salinity supply of Labrador coastal and shelf waters and saline inflow from the Gulf Stream while the flow exiting the region forms the eastward flow out of the area described by Pickart et al. (1999). The most “realistic” of the modeled flow regimes suggests a cyclonic circulation within the slope sea including some recirculation in the western portion. The relevant issue with respect to the observed slope jet is that the westward flow for most of the slope sea is confined to a “western boundary layer” that is not resolved in the model but which in the most realistic case is required to transport 2.6Sv to the west to close the circulation. This 2.6 Sv is remarkably close to the 2.5 Sv of estimated cumulative westward transport of the slope jet in Figure 9. Whether this is pure coincidence is difficult to determine at this point. Another aspect of this simple model is that since the curl of the wind stress is assumed to force the gyre circulation, the transport of the boundary current should be dependent on the strength of the winds. Figure 12 shows that the slope jet has a substantial seasonal cycle with the largest transports in the spring. Figure 23 shows the seasonal dependence of the pseudo-wind stress curl over the slope sea between Cape Hatteras and the Grand Banks based upon the ECMWF 40 year reanalysis 10 m monthly mean wind fields. The wind stress curl amplitudes computed from the ECMWF reanalysis over the slope sea are somewhat smaller than those computed from COADS winds by Ehret and O’Brien (1989) and about half that assumed by Csanady and Hamilton (1988). However, if we concentrate on the seasonal dependence on the ECMWF estimate of the wind stress curl there is clearly a substantial seasonal signal with a maximum positive curl of about $1.7 \times 10^5 \text{ m s}^{-2}$ occurring during the winter and a small negative curl in late summer and early fall. The Csanady

and Hamilton analysis scales the slope sea transports by the wind stress curl so that we would expect the gyre to virtually disappear in the summer months and our observations would appear to confirm this prediction. If this seasonal variation in the curl is responsible for the variation in the slope current then there is a lag of a month or more between the wind and the currents which would correspond to the spinup time for the gyre. Thus, on a seasonal scale it would appear that the slope sea currents vary primarily due to variable wind forcing while on interannual time scales the analysis of the currents and surface water properties of Figures 20 and 21 suggest a thermohaline competition between inflow from the north and south (Rossby et al., 2005).

The data collected during the Oleander Project have added a unique perspective of the structure and variability of the shelf water/slope water front, the shelfbreak jet and the northern portion of the slope sea gyre. On short time scales the region is highly variable while on longer time scales the regional currents are impacted by atmospheric and thermohaline processes. Gaining an understanding of the salient processes in such an environment requires long-term and detailed measurements. A singular advantage of volunteer observing ship programs is the compilation of data of long duration and through regions, conditions and seasons that would not otherwise be accessible. The more than 25 years of measurements gathered during the *Oleander* program so far cover several oceanographically critical areas and represent a particularly fine example of what is possible.

Acknowledgements

The long-term observational program that has been carried out on the CMV *Oleander* owes an enormous debt of gratitude to the Bermuda Container Lines as well as the forbearance of Captains Vrolyk, Van der Westeringh and Pye, and the ship's engineers and crew. The ADCP data collection itself was made possible through the patient efforts of George Schwartze and Sandra Fontana who were responsible for the maintenance of the system and the collection, processing and archiving of the seemingly never-ending stream of data from the project. The ADCP data collection started under the auspices of NOAA's North Atlantic Climate Change Program (NA16RC0523), was supported for a year by the Office of Naval Research (N000149910064) and then for the past 7 years support has been provided by the National Science Foundation (OCE9819724 and OCE0241654). The analysis presented here was supported by National Science Foundation (OCE0117653).

References

- Aikman, F., H.W. Ou, and R. W. Houghton (1988), Current variability across the New England continental shelf-break and slope. *Cont. Shelf Res.*, 8, 625-652.
- Barth, J.A., D. Bogucki, S.D. Pierce, P.M. Kosro (1998), Secondary circulation associated with a shelfbreak front. *Geophys. Res. Lett.*, 25, 2761-2764.
- Barth, J.A., D. Hebert, A.C. Dale, D.S. Ullman (2004) Direct observations of along-isopycnal upwelling and diapycnal velocity at a shelfbreak front. *J. Phys. Oceano.*, 34, 543-565.

Beardsley, R.C., C.N. Flagg (1976), Water structure, mean currents, and shelf-water/slope-water front on the New England continental shelf, in: *Seventh Liege Colloquim on Ocean Hydrodynamics*, *Societe Royale des Sciences*, edited by J.C.J. Nihoul, pp 209-226.

Beardsley, R.C., D.C. Chapman, K.H. Brink, S.R. Ramp, R. Schlitz (1985.), The Nantucket Shoals Flux Experiment (NSFE79). Part I, A basic description of the current and temperature variability. *J. Phys. Oceano.*, 15, 713-748.

Bigelow, H.B. (1933), Studies of the waters on the continental shelf, Cape Cod to Chesapeake Bay, I, The cycle of temperature. *Papers in Physical Oceanography and Meteorology*, 2, 1-135.

Bigelow, H.B., M. Sears (1935), Studies of the waters on the continental shelf, Cape Cod to Chesapeake Bay, II, Salinity. *Papers in Physical Oceanography and Meteorology*, 4, 1-94.

Biscaye, P.E., C.N. Flagg, P.G. Falkowski (1994), The Shelf Edge Exchange Processes experiment, SEEP-II: an introduction to hypotheses, results, and conclusions. *Deep-Sea Res., Part II*, 41, 231-252.

Chapman, D.C. and R.C. Beardsley (1989), On the origin of the shelf water in the Middle Atlantic Bight. *J. Phys. Oceano.*, 19, 384-391.

Chapman, D.C. (1986), A simple model of the formation and maintenance of the shelf/slope front in the Middle Atlantic Bight. *J. Phys. Oceano.*, 16, 1273-1279.

Chapman, D.C. (2002), Sensitivity of a model shelfbreak front to the parameterization of vertical mixing. *J. Phys. Oceano.*, 32, 3291-3298.

Chapman, D.C., S.J. Lentz. 1994. Trapping of a coastal density front by the bottom boundary layers. *J. Phys. Oceano.*, 24, 1464-1479.

Chapman, D.C., S.J. Lentz. 1997. Adjustment of stratified flow over a sloping bottom. *J. Phys. Oceano.*, 27, 340-356.

Csanady, GT, and P. Hamilton (1988), Circulation of slopewater. *Cont. Shelf Res.*, 8, 565–624.

Curry, R.G. (1996), Hydrobase: A database of hydrographic stations and tools for climatological analysis, Tech. Rep. WHOI-96-01, 50 pp, Woods Hole Oceanographic Institution, Woods Hole, Mass.

Dickey, T.D. and A.J. Williams (2001), Interdisciplinary ocean process studies on the New England Shelf. *J. Geophys. Res.*, 106, 9427-9434.

Drinkwater, K. F., D. G. Mountain, A. Herman (2005), Variability in the slope water properties off eastern North America and their effects on the adjacent shelves. *J. Geophys. Res.*, (submitted).

- Dunn, M. (2002), A Description of the Barotropic Tide On Georges Bank Based Upon Five Years of Shipboard ADCP Observations. MS Thesis, 56pp, Marine Environmental Science, Stony Brook University, Stony Brook, New York,
- Ehret, L.L and J.J. O'Brien (1989), Scales of North Atlantic wind stress curl determined from the Comprehensive Ocean-Atmosphere Data Set. *J. Geophys. Res.*, *94*, 831-841.
- Flagg, C.N., G.Schwartz, E. Gottlieb, and T. Rossby (1997), Operating an acoustic Doppler current profiler (ADCP) aboard a container vessel. *J. Atmos. and Oceanic Tech.*, *15*, 257–271.
- Frantantoni, P.S. and R.S. Pickart (2003), Variability of the shelf break jet in the Middle Atlantic Bight: Internally or Externally Forced? *J. Geophys. Res.*, *108*, doi:10.1029/2002JC001326.
- Frantantoni, P.S., R.S. Pickart, D.J. Torres, A. Scotti (2001), Mean structure and dynamics of the shelfbreak jet in the Middle Atlantic Bight during fall and winter. *J. Phys. Oceano.*, *31*, 2135-2156.
- Gatien, M.G. (1976), A study in the slope water region south of Halifax. *J. Fish. Res. Board Can.*, *33*, 2213-2217.
- Gawarkiewicz, G., D.C. Chapman (1991), Formation and maintenance of shelfbreak fronts in an unstratified flow. *J. Phys. Oceano.*, *21*, 1225-1239.
- Gawarkiewicz, G., D.C. Chapman (1992), The role of stratification in the formation and maintenance of shelf-break fronts. *J. Phys. Oceano.*, *22*, 753-772.
- Gawarkiewicz, G., K.H. Brink, F. Bahr, R.C. Beardsley, M. Caruso and J.F. Lynch (2004), A large-amplitude meander of the shelfbreak front during summer south of New England: Observations from the shelfbreak PRIMER experiment. *J. Geophys. Res.*, *109*, doi:10.1029/2002JC001468.
- Greene, C.H. and A.J. Pershing (2003) The flip-side of the North Atlantic Oscillation and modal shifts in slope-water circulation patterns. *Limnol. Oceanogr.*, *48*, 2003, 319–322.
- Hendry, R. (2001), Slope water circulation and sea level. CSAS Proceedings of the Workshop on “The Northwest Atlantic Ecosystem – A basin-scale approach”, 21-23, June 2001.
- Houghton, R.W. (1995), The bottom boundary layer structure in the vicinity of the Middle Atlantic Bight shelf-break front. *Cont. Shelf Res.*, *15*, 1173-1194.
- Houghton, R.W. (1997), Lagrangian flow at the foot of the shelfbreak front using a dye tracer injected into the bottom boundary layer. *Geophys. Res. Lett.*, *24*, 2035-2038.
- Houghton, R.W. and M. Visbeck (1998), Upwelling and convergence in the Middle Atlantic Bight shelfbreak front. *Geophys. Res. Lett.*, *25*, 2765-2768.

- Linder, C.A., G. Gawarkiewicz (1998), A climatology of the shelfbreak front in the Middle Atlantic Bight. *J. Geophys. Res.*, *103*, 18405-18423.
- Loder, J.W., B. Petrie, G. Gawarkiewicz (1998), The coastal ocean off northeastern North America: A large-scale view, in *The Sea, 11*, edited by A.R. Robinson and K.H. Brink, pp. 105-133, John Wiley & Sons, New York..
- Lozier, M.S., M.S. Reed, G. Gawarkiewicz (2002), Instability of a shelfbreak front. *J. Phys. Oceano.*, *1*, 924-944.
- Marra, J., R.W. Houghton, C. Garside (1990) Phytoplankton growth at the shelf-break front in the Middle Atlantic Bight. *J. Marine Res.*, *48*, 851-868.
- Moody, J. A., B. Butman, R. C. Beardsley, W. S. Brown, P. Daifuku, J. D. Irish, D. A. Mayer, H. O. Mofjeld, B. Petrie, S. Ramp, P. Smith, and W. R. Wright (1984), Atlas of Tidal Elevations and Current Observations on the Northeast American Continental Shelf and Slope. *U. S. Geol. Surv. Bull.*, *1611*, 122pp.
- O'Reilly, J.E., C. Evans-Zetlin, D.A. Busch (1987), Primary Production, in: *Georges Bank*, edited by R. Backus, pp. 220-233, M.I.T. Press, Cambridge, MA.
- Pershing, A.J., C.H. Greene, C. Hannah, D. Sameoto, E. Head, D.G. Mountain, J.W. Jossi, and M.C. Benfield (2001) Oceanographic responses to climate in the northwest Atlantic., *Oceanography*, *14*, 76-82.
- Pickart, R.S., T.K. McKee, D.J. Torres, and S.A. Harrington (1999), Mean Structure and Interannual Variability of the Slopewater system south of Newfoundland. *J. Phys. Oceano.*, *29*, 2541-2558.
- Pickart, R.S. (2000), Bottom boundary layer structure and detachment in the Shelfbreak Jet of the Middle Atlantic Bight. *J. Phys. Oceano.*, *30*, 2668-2686.
- Rossby, T. and R. Benway (2000), Slow variations in the mean path of the Gulf Stream east of Cape Hatteras. *Geo. Res. Lett.*, *27*, 117-120.
- Rossby T., C. N. Flagg, and K. Donohue (2005), Interannual variations in upper-ocean transport by the Gulf Stream and adjacent waters between New Jersey and Bermuda, *J. Marine Res.*, *63*, 203-226.
- Ryan, J.P., J.A. Yoder, and P.C. Cornillon (1999), Enhanced chlorophyll at the shelfbreak of the Mid-Atlantic Bight and Georges Bank during the spring transition. *Limnol. Oceanogr.*, *44*, 1-11.
- Ryther, J.H. and C.S. Yentsch (1958), Primary production of continental shelf waters off New York. *Limnol. and Oceano.*, *3*, 327-335.

Smith, P.C., R.W. Houghton, R.G. Fairbanks, and D.G. Mountain (2001), Interannual variability of boundary fluxes and water mass properties in the Gulf of Maine and on Georges Bank: 1993-1997. *Deep Sea Res. II*, 48, 37-70.

Verity, P.G., J.E. Bauer, C.N. Flagg, D.J. DeMaster and D.J. Repeta (2002), The Ocean Margins Program: an interdisciplinary study of carbon sources, transformations, and sinks in a temperate continental margin system. *Deep-Sea Res. Part II*, 49, 4273-4296.

Walsh, J.J., P.E. Biscaye, and G.T. Csanady (1988), The 1983-1984 Shelf Edge Exchange Processes (SEEP) – I experiment: hypotheses and highlights. *Cont. Shelf Res.*, 8, 435-456.

Wright, W.R. (1976), The limits of shelf water south of Cape Cod. *J. Marine Res.*, 34, 1-14.

Yankovsky, A.E., D.C. Chapman (1997), A simple theory for the fate of buoyant coastal discharges. *J. Phys. Oceano.*, 27, 1386-1401.

Figure Captions

Figure 1. Spatial distribution of the MV Oleander's ADCP data in the shelf/slope front region and the along-track distance from Ambrose Light that is used as a reference coordinate.

Figure 2. The shows the location of warm ring centers from 1991 through 2001 that passed through the study area.

Figure 3. Available velocity data distribution as a function of offshore distance and depth based upon 2 km x 8 m binned results.

Figure 4. Near-surface temperature and Along- and Offshore ADCP velocity section for July 12, 1997.

Figure 5. Near-surface temperature and Along- and Offshore ADCP velocity section for December 9, 1995

Figure 6. Near-surface temperature and Alongshore ADCP velocity section for May/June 1996 showing the temporal variability that is characteristic of the region.

Figure 7. a. Sample mean along- and offshore velocity sections from 2km x 8m binned velocity data from 282 warm-ring free transits of the shelfbreak region. b. Standard errors for the mean along- and offshore velocity sections from 2km x 8m binned velocity data from 282 warm-ring free transits of the shelfbreak region.

Figure 8. 2km binned mean upper layer (14 to 52m) velocity vectors and current ellipses from the 282 warm-ring free transits of the shelfbreak region. Every fourth ellipse is shown.

Figure 9. Alongshore transports of the shelfbreak jet and slope current above 400m.

Figure 10. Histograms of the offshore and vertical position of the high speed center of the shelfbreak jet. In the left panel the white bars represent the location of centers found above 200m, the grey bars those centers found above 100m and the black bars shows those centers found above 50m.

Figure 11, Mean structure of the shelfbreak jet in stream coordinates for those sections in which the highest speeds were shallower than 50m (see text). The vertical white line indicates the center of the jet.

Figure 12. Seasonal Eulerian mean alongshore currents, positive toward 225°.

Figure 13. Seasonal dependence of the vertically averaged upper layer currents between 22 and 54 m for each 2 km distance bin as determined from a least-square fit to a mean plus annual and semi-annual components.

Figure 14. Upper layer (14 to 54 m), long-term current fluctuations after the removal of the mean and seasonal fluctuations. The data were averaged into 60-day intervals and low-passed filter with a one-year half-power point.

Figure 15. Upper ocean temperature and salinity anomalies from monthly XBT and surface salinity observations from the CMV Oleander carried out by the NMFS/Northeast Fisheries Science Center, Narragansett, RI. The data have been binned into 10km intervals along the Oleander track between New York and the mean position of the Gulf Stream. The area marked by the dashed box indicates the overlapping time and space of the Oleander ADCP data discussed in this paper.

Figure 16. Time series of upper ocean alongshore current, temperature and salinity anomalies from the approximately center of the shelfbreak jet and slope current at 160km (blue) and 260km (red), respectively, from Ambrose Light. Note that the vertical axes for the temperature and salinity anomalies have been reversed to emphasize the relationship between positive (southwestward) alongshore flow and subsequent cold/fresh anomalies and vice versa.

Figure 17. Seasonal dependence of the pseudo-wind stress curl over the slope sea between Cape Hatteras and the Grand Banks from the ECMWF 40 year reanalysis of monthly mean winds at 10m.

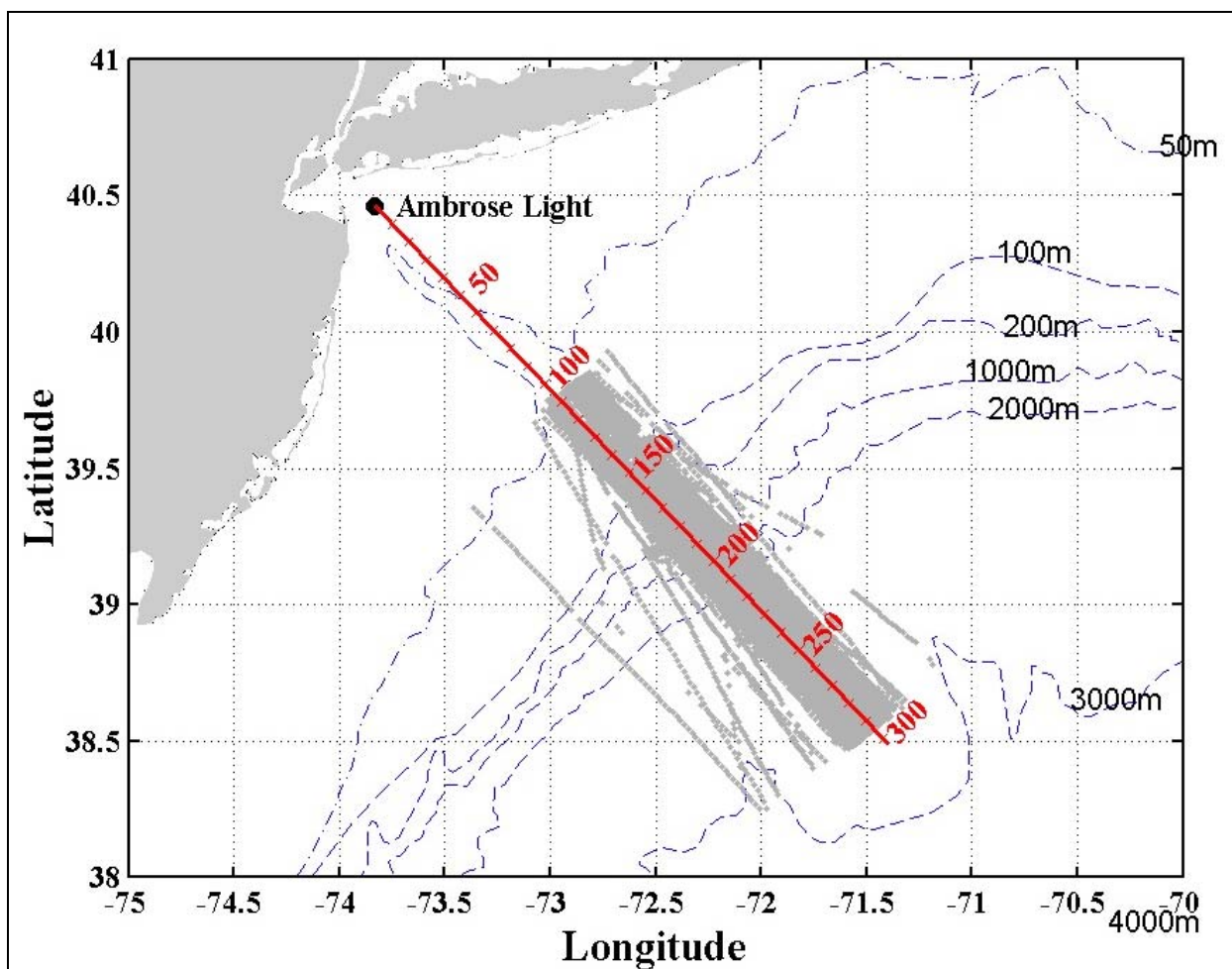
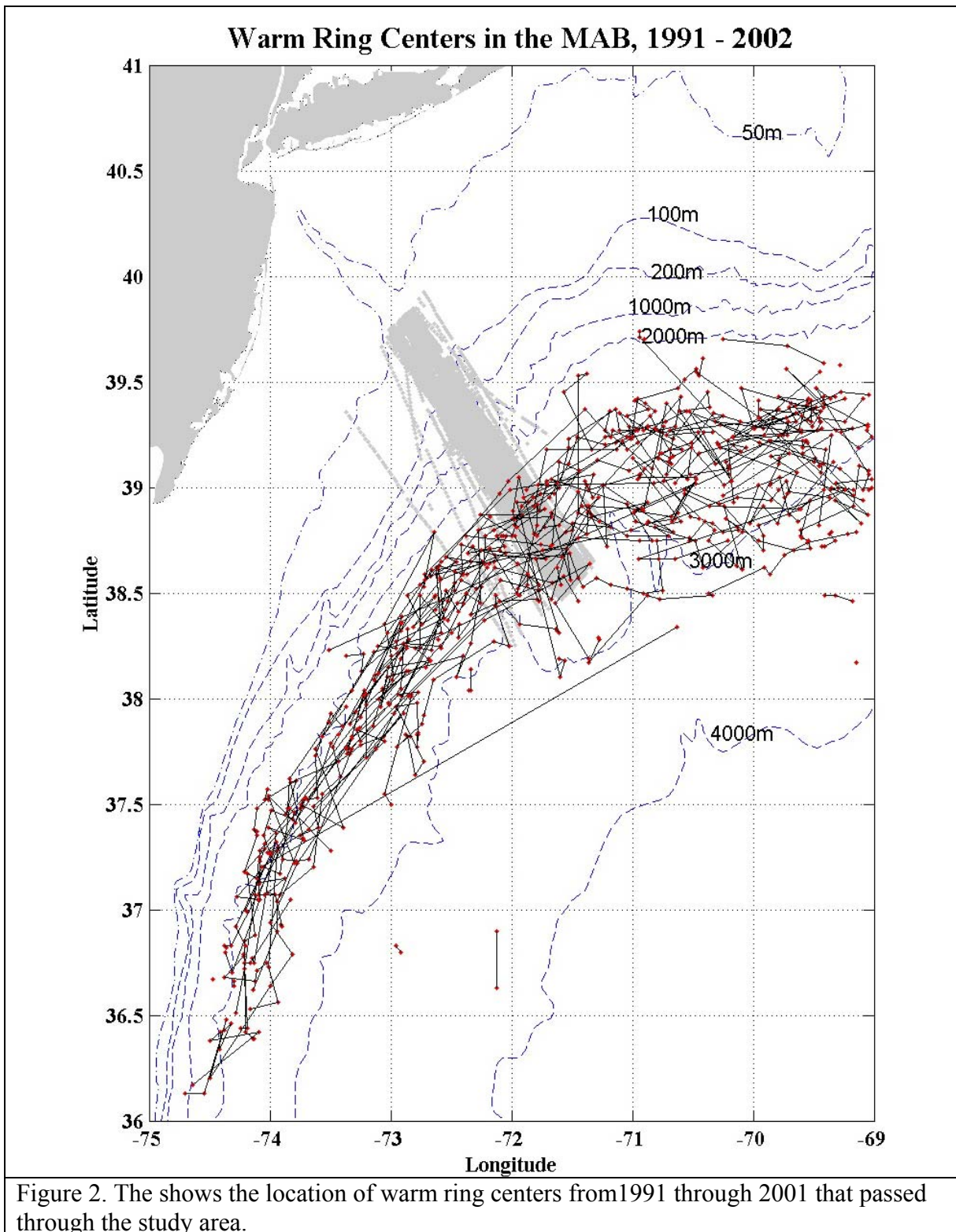
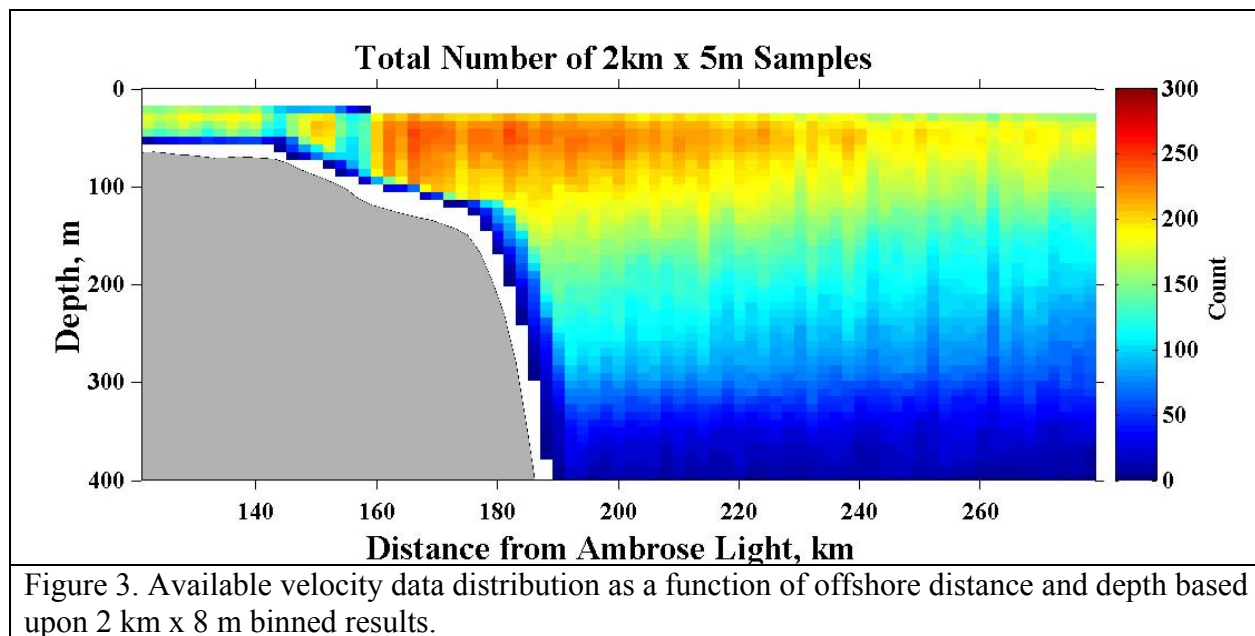
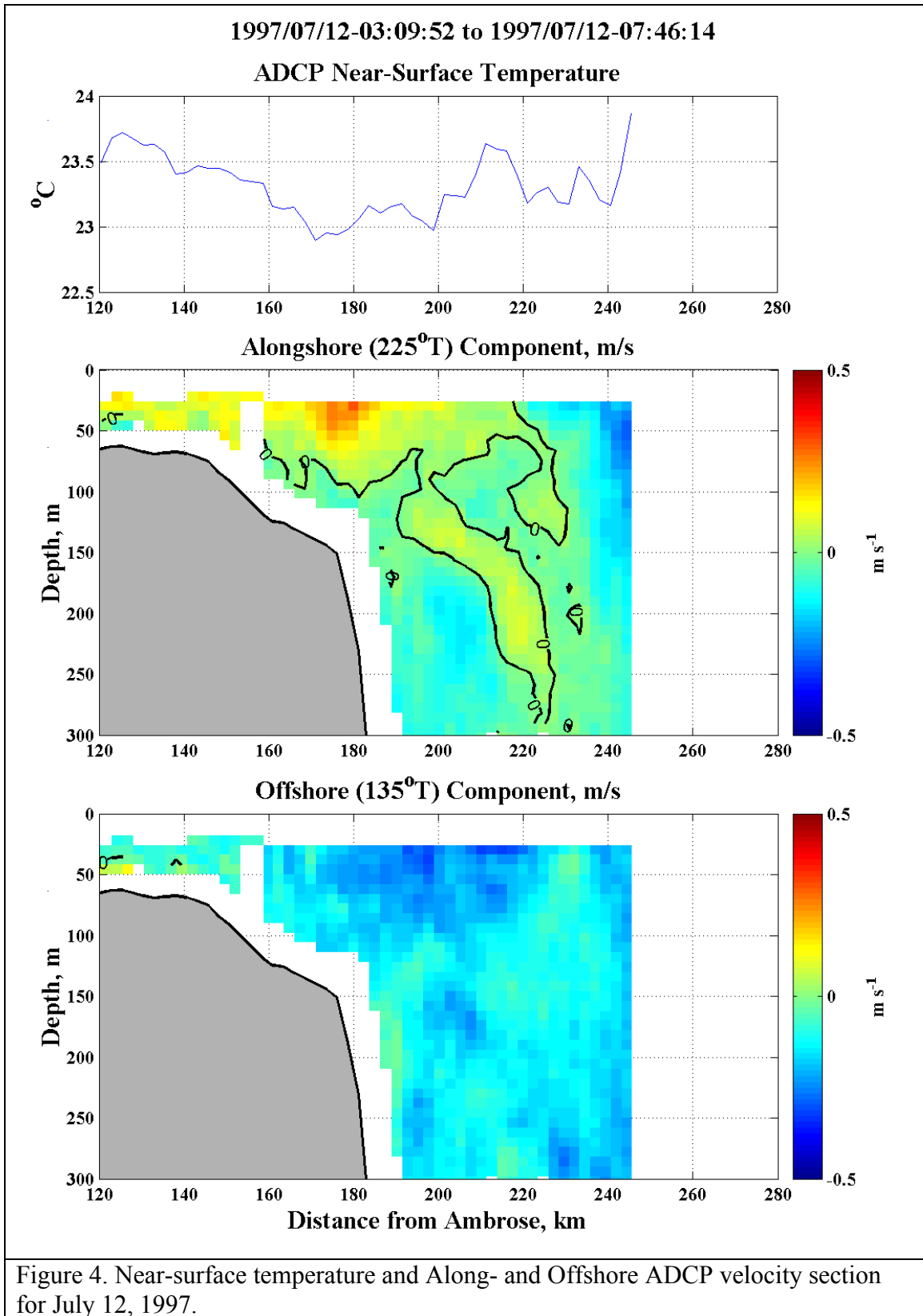
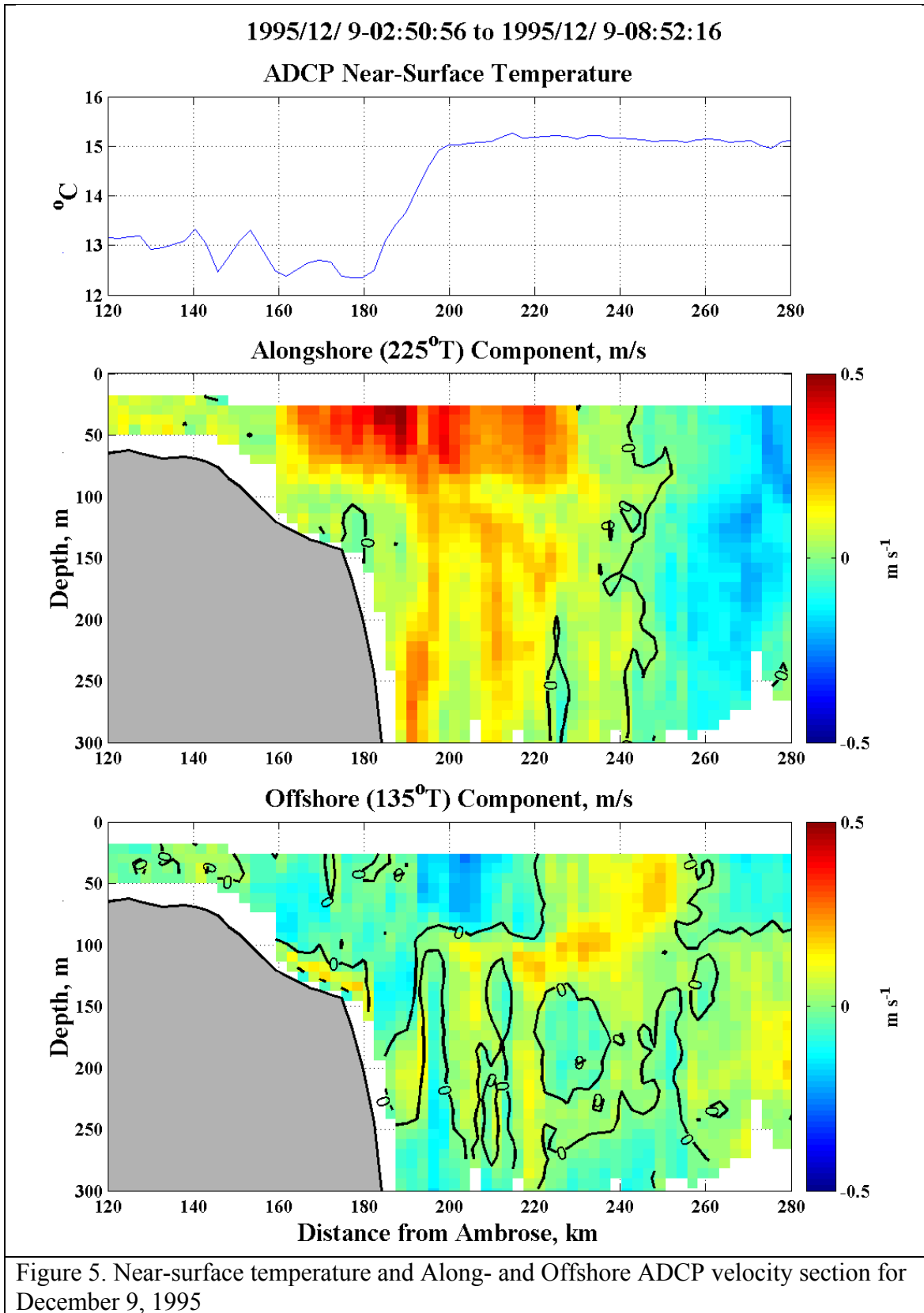


Figure 2. Spatial distribution of the MV Oleander's ADCP data in the shelf/slope front region and the along-track distance from Ambrose Light that is used as a reference coordinate.









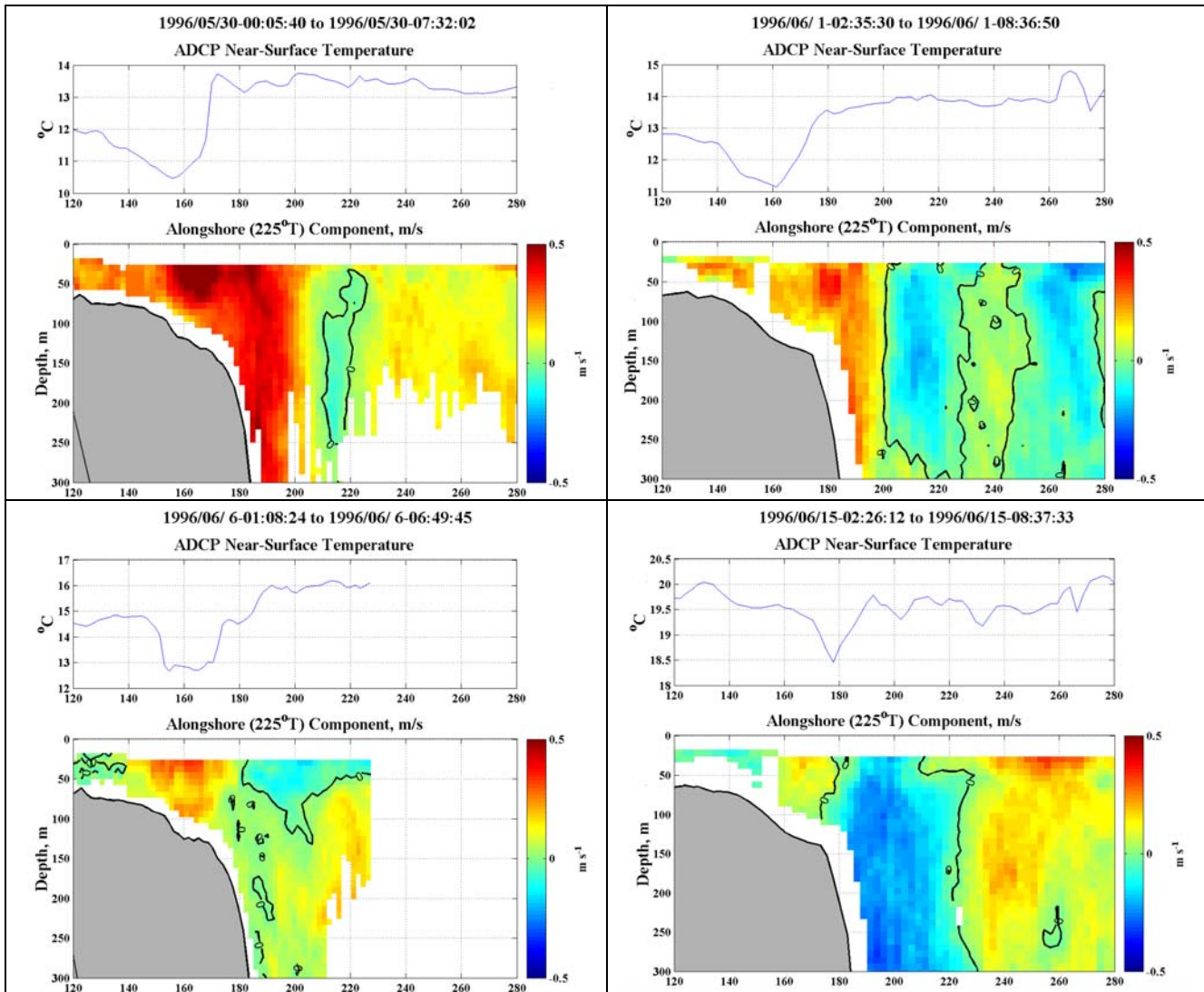


Figure 6. Near-surface temperature and Alongshore ADCP velocity section for May/June 1996 showing the temporal variability that is characteristic of the region.

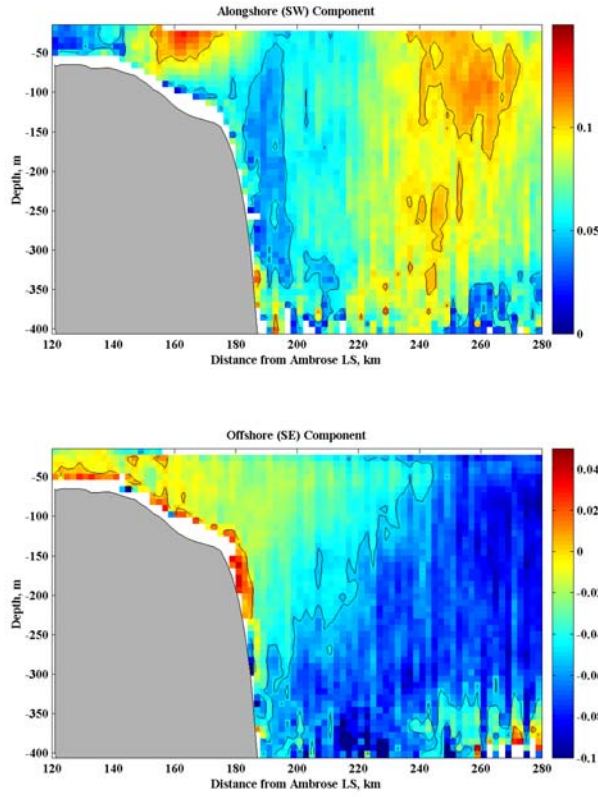


Figure 7a. Sample mean along- and offshore velocity sections from 2km x 8m binned velocity data from 282 warm-ring free transits of the shelfbreak region.

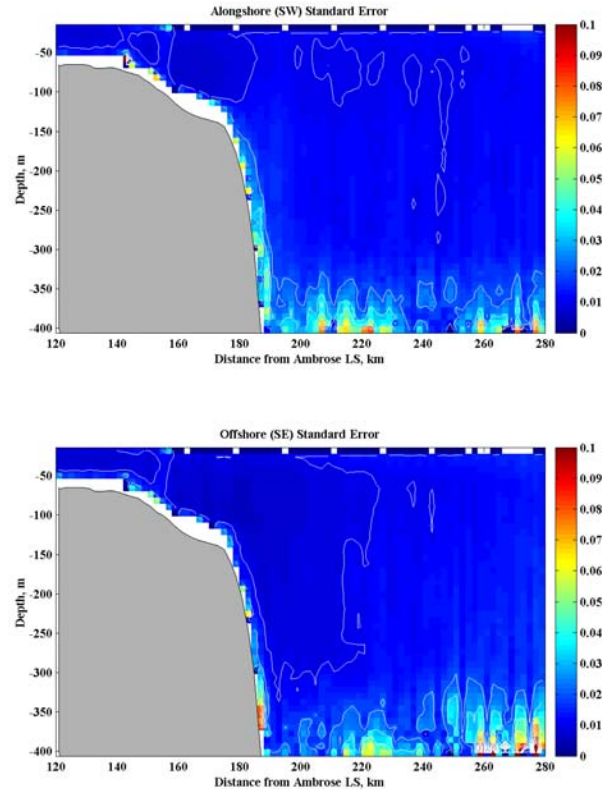
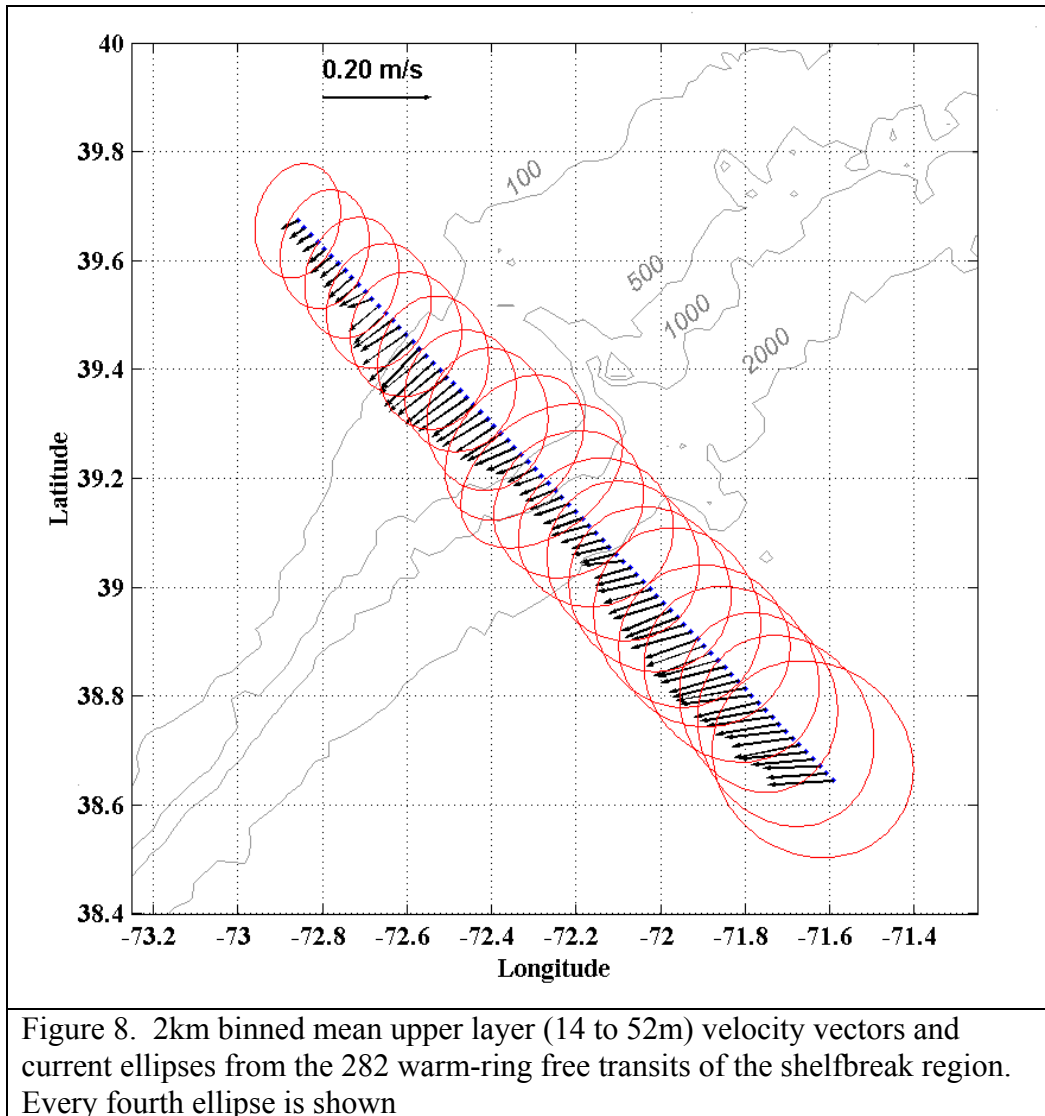


Figure 7b. Standard errors for the mean along- and offshore velocity sections from 2km x 8m binned velocity data from 282 warm-ring free transits of the shelfbreak region.



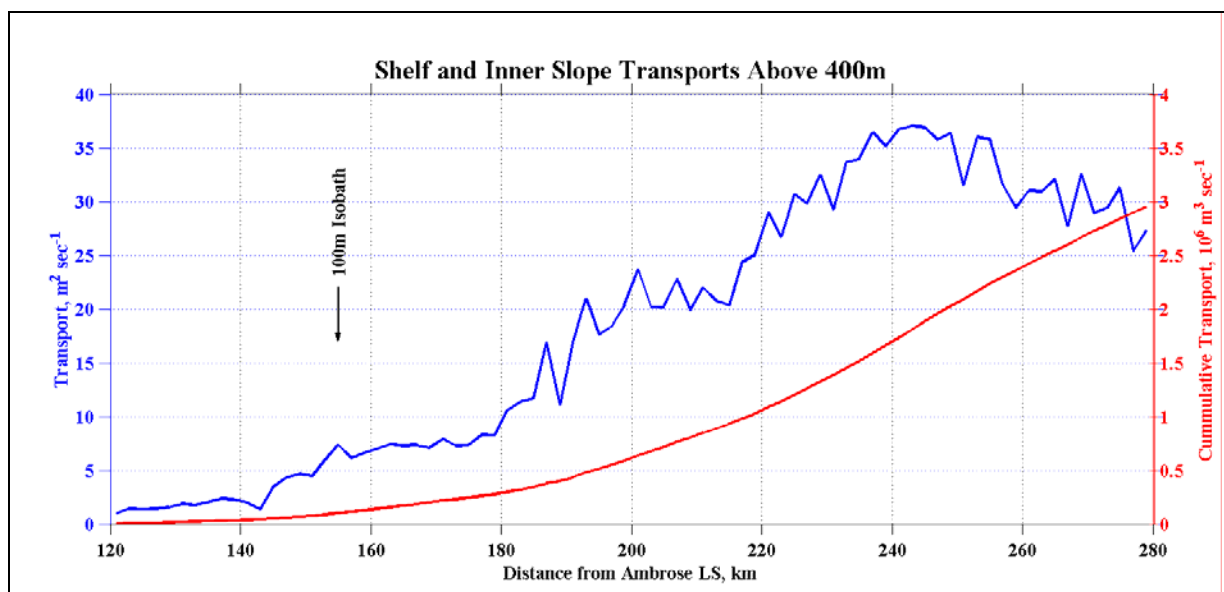


Figure 9. Alongshore transports of the shelfbreak jet and slope current above 400m.

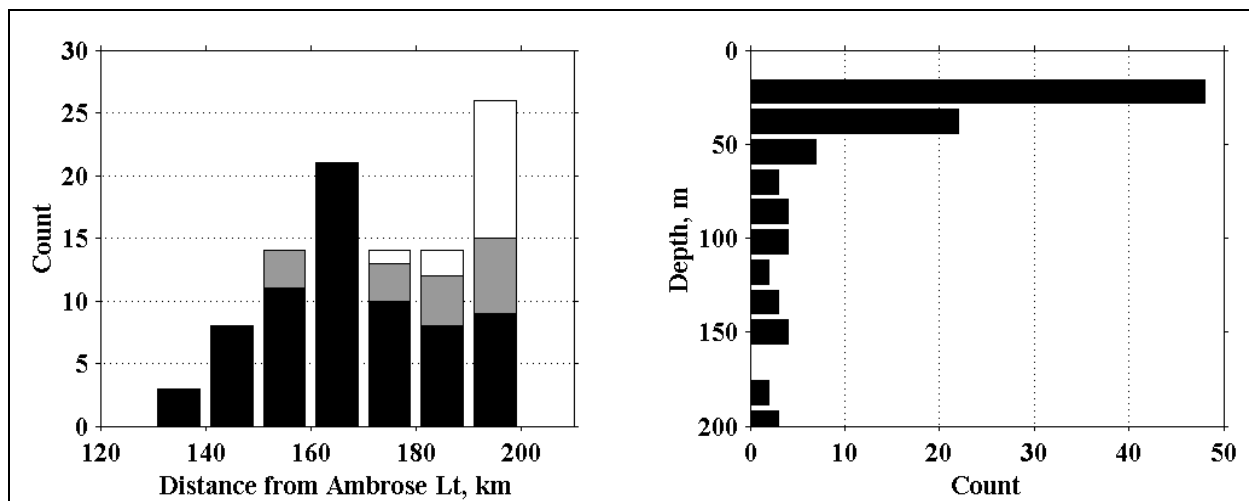


Figure 10. Histograms of the offshore and vertical position of the high speed center of the shelfbreak jet. In the left panel the white bars represent the location of centers found above 200m, the grey bars those centers found above 100m and the black bars shows those centers found above 50m.

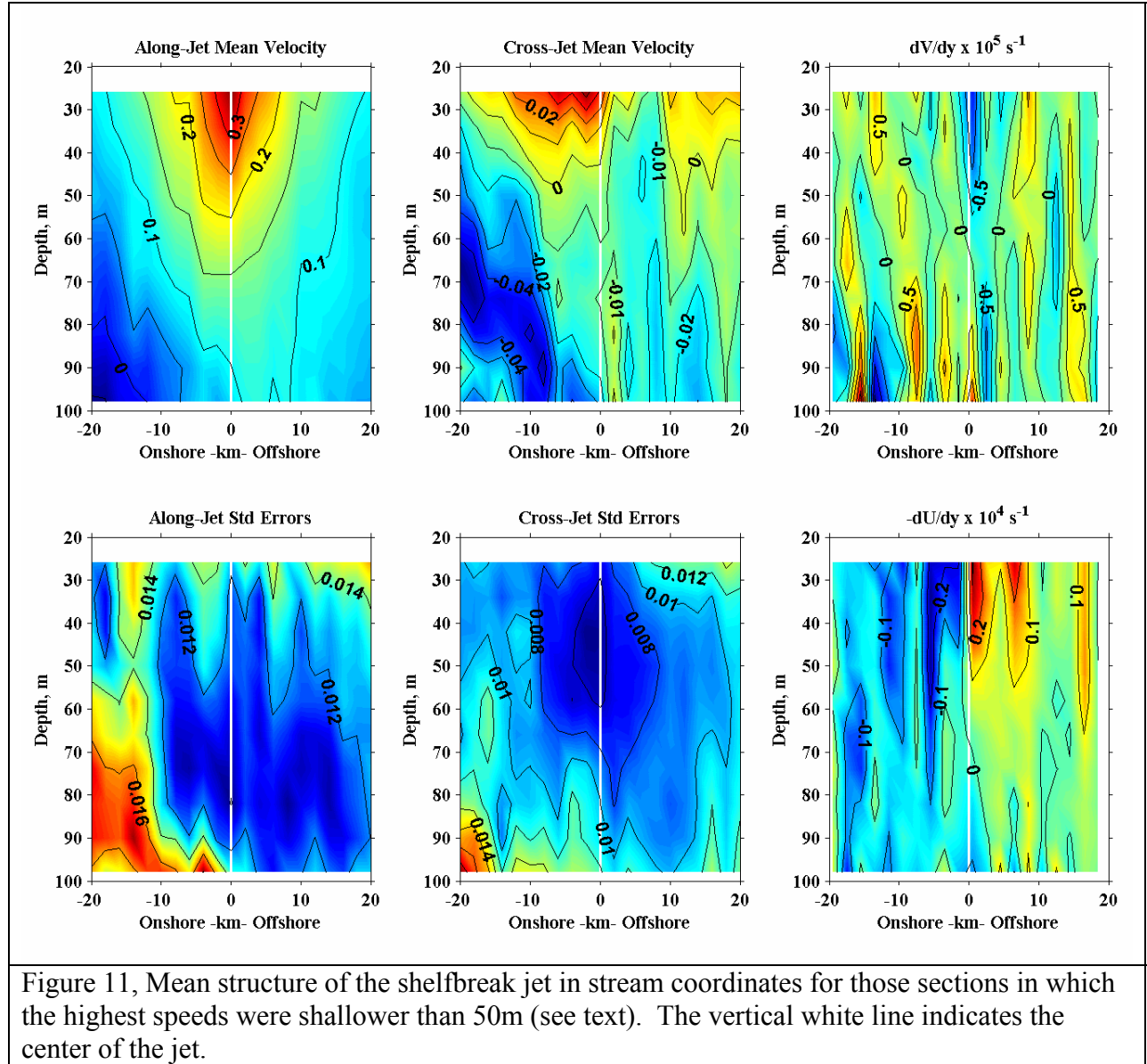


Figure 11, Mean structure of the shelfbreak jet in stream coordinates for those sections in which the highest speeds were shallower than 50m (see text). The vertical white line indicates the center of the jet.

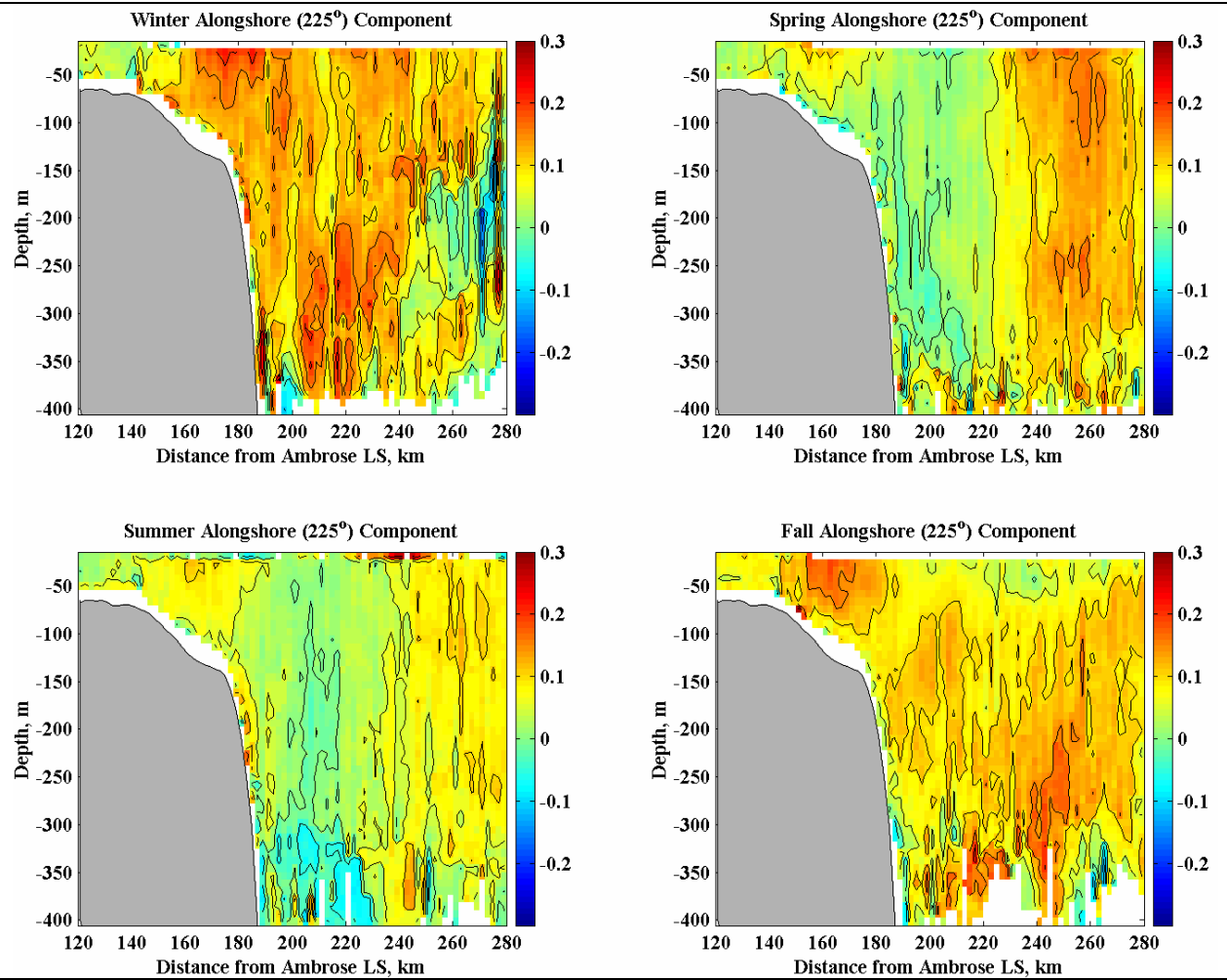
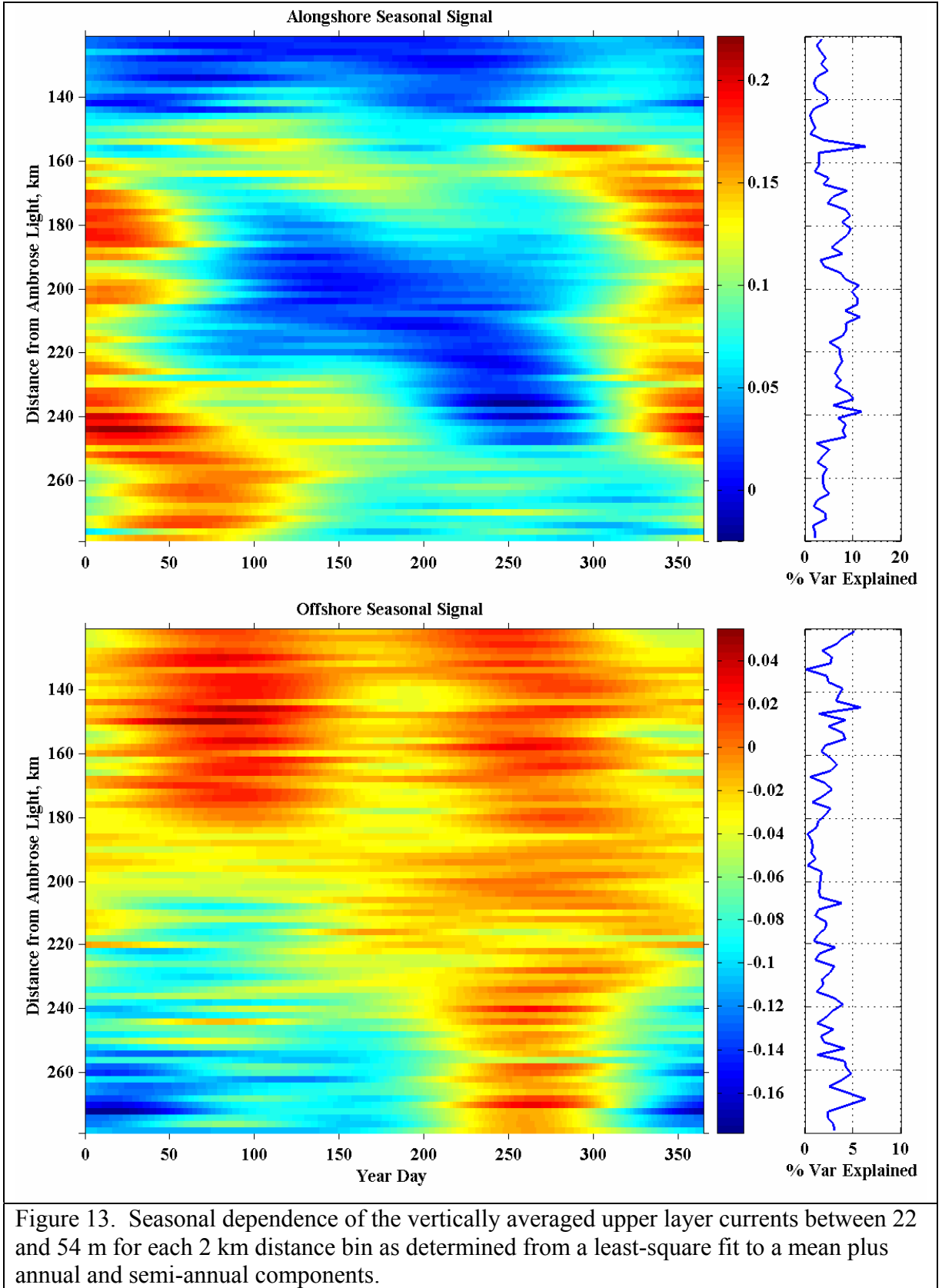
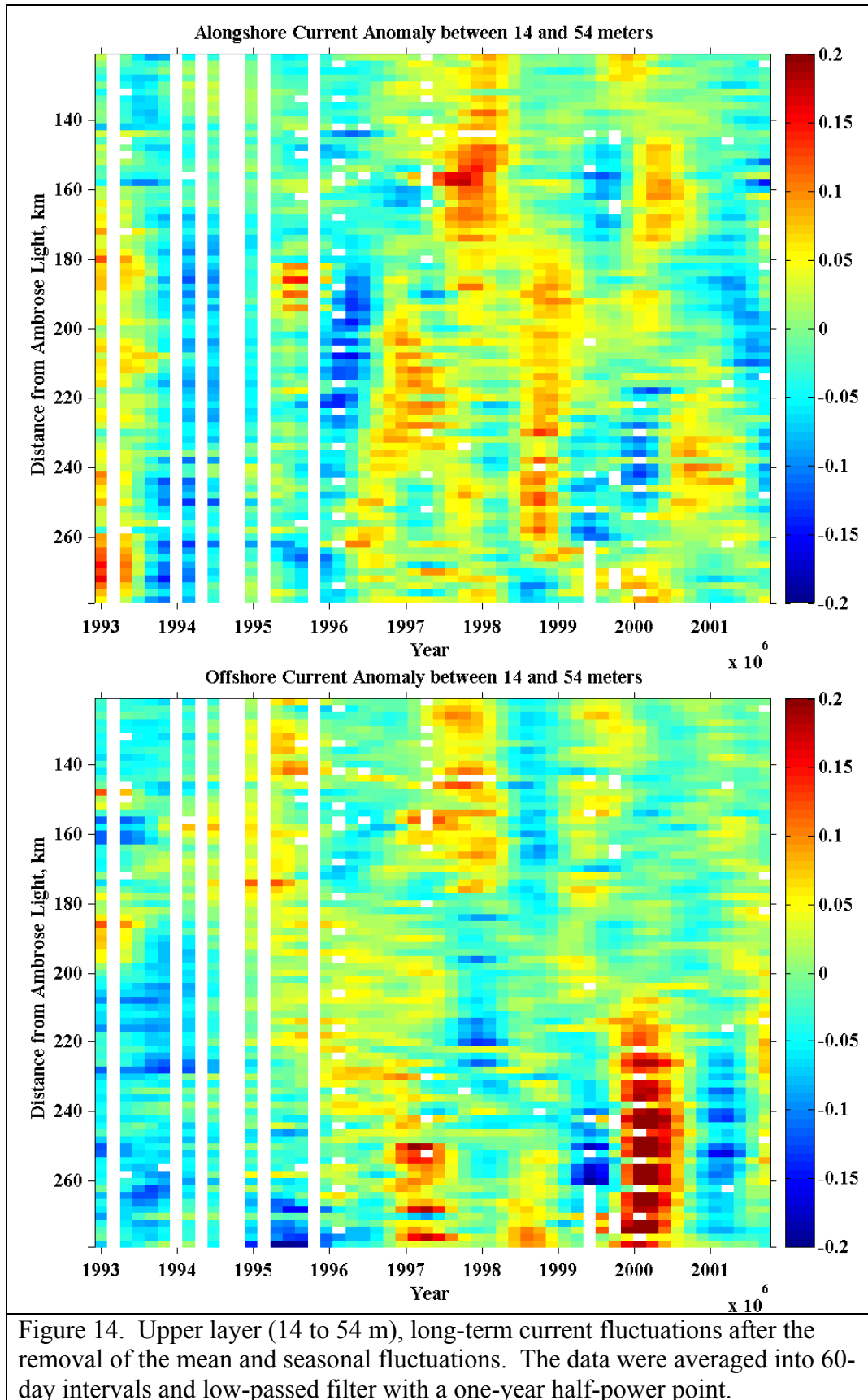
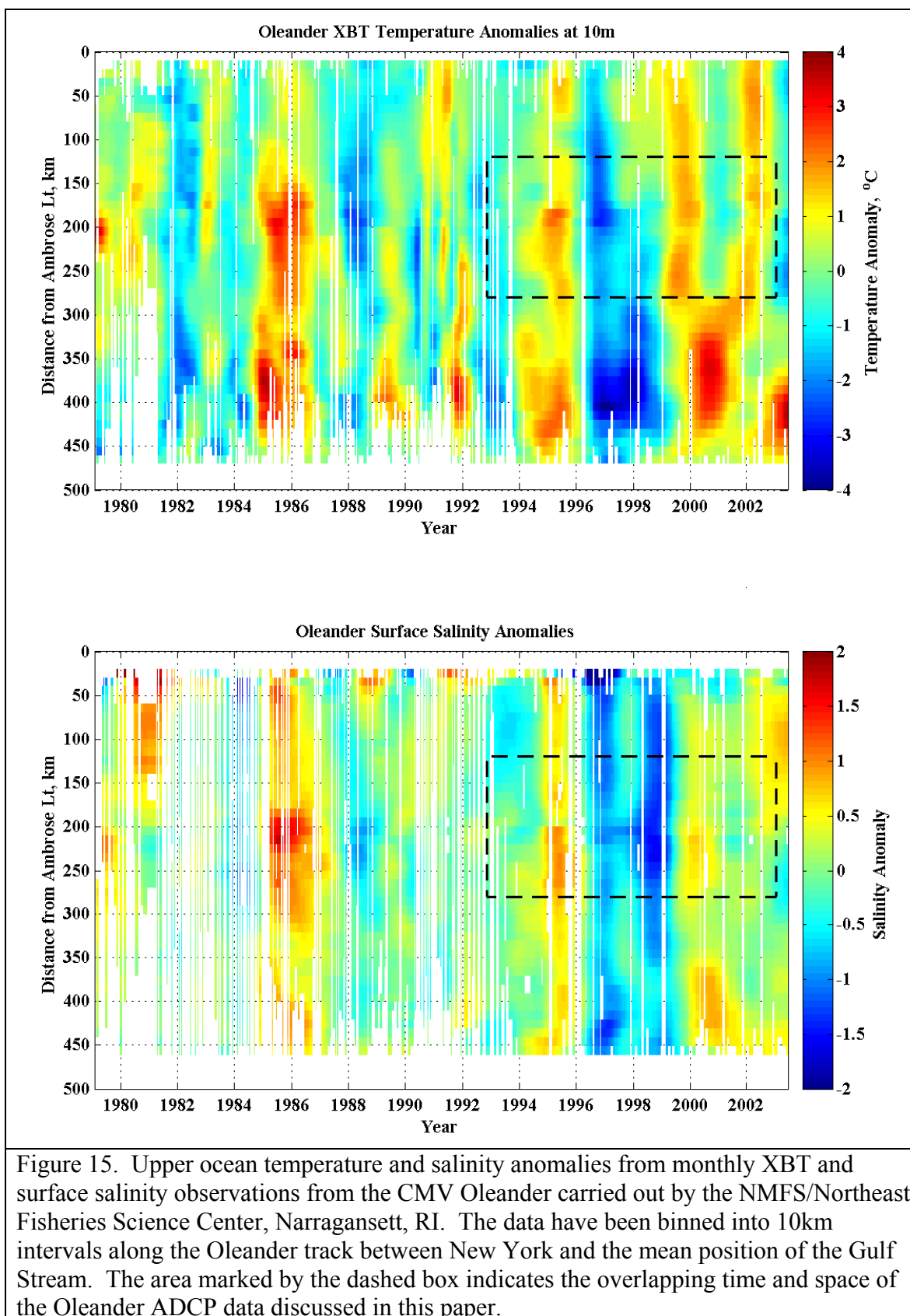


Figure12. Seasonal Eulerian mean alongshore currents, positive toward 225°.







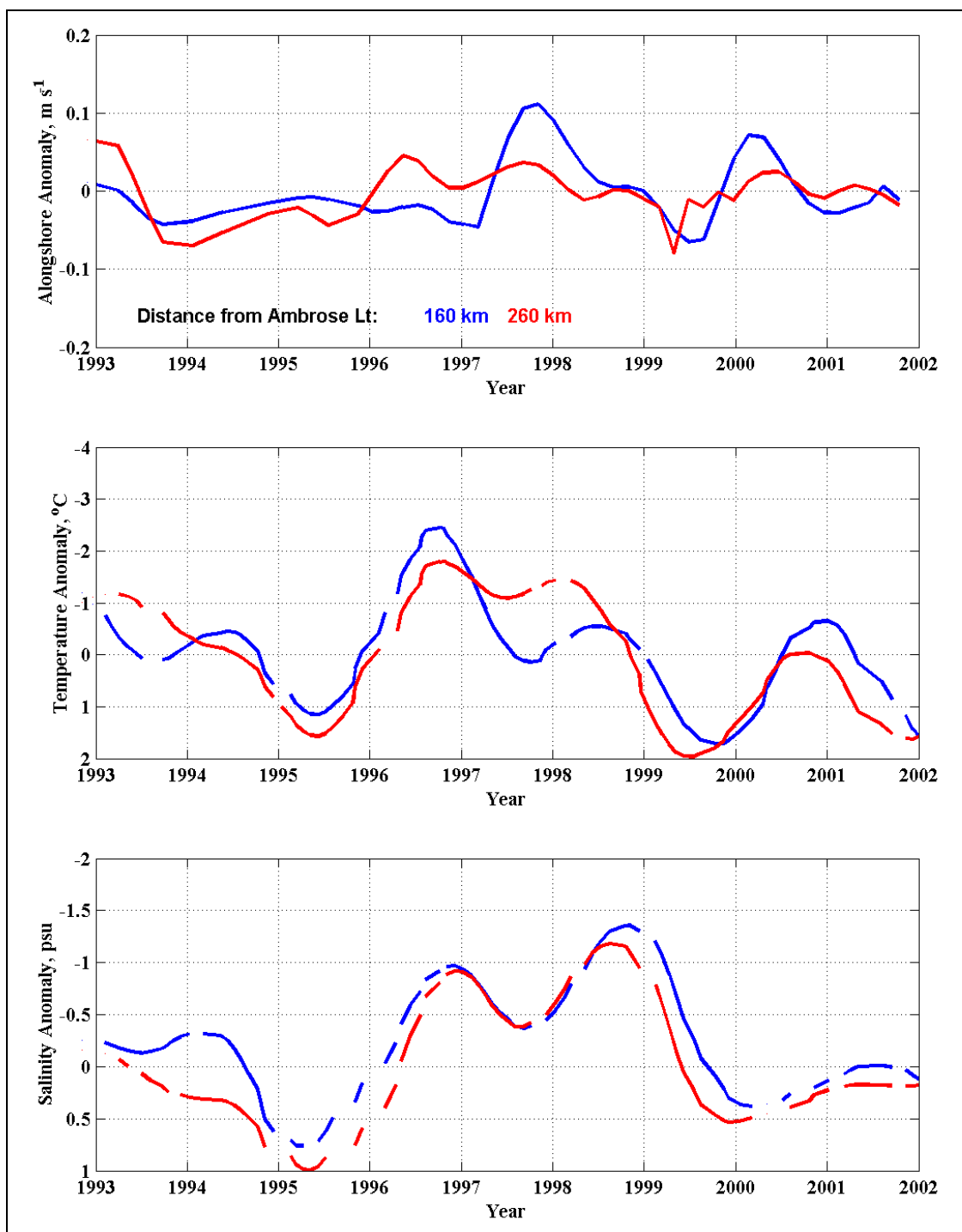


Figure 16. Time series of upper ocean alongshore current, temperature and salinity anomalies from the approximately center of the shelfbreak jet and slope current at 160km (blue) and 260km (red), respectively, from Ambrose Light. Note that the vertical axes for the temperature and salinity anomalies have been reversed to emphasize the relationship between positive (southwestward) alongshore flow and subsequent cold/fresh anomalies and vice versa.

